Top Curr Chem (2012)
DOI: 10.1007/128_2012_355

Volatility and Aging of Atmospheric Organic Aerosol

Neil M. Donahue, Allen L. Robinson, Erica R. Trump, Ilona Riipinen, and Jesse H. Kroll

Abstract Organic-aerosol phase partitioning (volatility) and oxidative aging are inextricably linked in the atmosphere because partitioning largely controls the rates and mechanisms of aging reactions as well as the actual amount of organic aerosol. Here we discuss those linkages, describing the basic theory of partitioning thermodynamics as well as the dynamics that may limit the approach to equilibrium under some conditions. We then discuss oxidative aging in three forms: homogeneous gas-phase oxidation, heterogeneous oxidation via uptake of gas-phase oxidants, and aqueous-phase oxidation. We present general scaling arguments to constrain the relative importance of these processes in the atmosphere, compared to each other and compared to the characteristic residence time of particles in the atmosphere.

Keywords Aerosols · Atmospheric Chemistry · Multiphase Chemistry

N.M. Donahue (✉), A.L. Robinson and E.R. Trump
Carnegie Mellon University Center for Atmospheric Particle Studies, Pittsburgh, PA, USA
e-mail: nmd@andrew.cmu.edu

I. Riipinen
Department of Applied Environmental Science and Bert Bolin Centre for Climate Research, Stockholm University, Stockholm, Sweden

Carnegie Mellon University Center for Atmospheric Particle Studies, Pittsburgh, PA, USA

J.H. Kroll
Department of Civil and Environmental Engineering, Massachusetts Institute of Technology, Cambridge, MA, USA

Department of Chemical Engineering, Massachusetts Institute of Technology, Cambridge, MA, USA

Contents

1 Introduction

Until very recently organic aerosol (OA) was commonly regarded as a mixture of non-volatile, non-reactive, primary organic aerosol (POA) [1, 2] augmented with a coating of secondary organic aerosol (SOA). POA particles were regarded as relatively non-volatile composites of organic compounds emitted by individual sources, such as biomass burning [3–5], gasoline [6–8] and diesel [1, 9] vehicles, food preparation [10–13], smoking [14], and numerous other small sources. SOA was regarded as an additional coating of secondary organic compounds formed via gas-phase oxidation of volatile organic carbon (VOC) precursors. Some of these reaction products evidently had a sufficiently low vapor pressure to condense onto pre-existing particles [15, 16]. Through a decade or so of research it became clear that SOA consisted of a mixture containing a large fraction of semi-volatile organic compounds that partitioned between the vapor and condensed phases based on well-established solution thermodynamics [17, 18].

This basic picture of organic aerosol was relatively well developed by the end of the 1990s. Chemical transport models were fed by inventories for POA emissions from a wide array of sources, and those emissions were treated in a variety of microphysics modules as effectively non-volatile and often chemically inert particles [19, 20]. SOA models evolved from relatively primitive treatments that simply converted a fixed fraction of VOC emissions into equally non-volatile secondary material (for example 12% of monoterpene emissions) to more sophisticated "two-product" representations that treated the equilibrium partitioning of surrogate species based on smog-chamber experiments [21–23]. Even today some global-scale models represent SOA as a fixed non-volatile fraction of VOC emissions [24, 25].

In most model representations of OA behavior, there was little if any consideration of long-term OA aging. With the realization that some OA could serve as relatively efficient cloud condensation nuclei [26–28] and also that soluble salts such as ammonium sulfate would condense onto even the most hydrophobic organic cores, many models added some form of ad hoc aging timescale, typically converting a "hydrophobic" organic mode into a "hydrophilic" organic mode with a fixed timescale (usually of order 2 days).

Recently this picture has been more or less turned upside down. We now recognize that most POA emissions are actually fairly volatile, while SOA (at least in the form found in the atmosphere) is not very volatile at all [29, 30]. There is some debate over the effective volatility of even "traditional" SOA formed in smog-chamber experiments (called "chamber SOA" hereafter) [31], but it is also clear that chamber SOA is often a poor match for the SOA observed in the atmosphere. At the same time, recent papers have raised questions about the physical state of OA particles. There is considerable evidence that some OA particles may exist in a glassy or semi-solid state [32–34], and there is some confusion about whether this glassy state invalidates the solution thermodynamics treatments that have been developed to date (it does not) and debate over whether the mixtures actually reach equilibrium (they may not).

Work in our groups over the past decade has focused on the hypothesis that the coupling of gas-particle partitioning and gas-phase oxidation chemistry plays a central role in the properties and evolution of organic aerosol in the atmosphere, and that a very large fraction of all organic carbon atoms found in ambient particles has been involved in gas-phase chemical reactions at some point during their stay in the atmosphere. Volatility, in other words, plays a central role in the aging of organic aerosol in the atmosphere.

This chapter will focus on the interplay between volatility and chemical aging as it relates to organic aerosol. We shall emphasize the role of gas-phase oxidation chemistry but address other mechanisms as well. That emphasis is not meant to suggest that other aging mechanisms are unimportant, but rather that this one is important. Many of those other processes are ably covered by other articles in this volume.

2 Background

Of a total flux of non-methane reduced organic compounds into the atmosphere of about 1,350 Tg year^{-1} [35, 36], only 10% or so leads to organic aerosol [25, 37]. However, less than 1% of the primary organic emissions into the atmosphere have a sufficiently low volatility to remain in the condensed phase under ambient conditions, so SOA formation must be a huge part (90% or more) of the OA story [38]. The straightforward fact is that only a small fraction of all organic compounds (by mass) in the atmosphere have what it takes to stay on or in a particle. That special property is low volatility, and most compounds acquire that low volatility via chemical transformation in the atmosphere.

It is important to develop a sense of scale for volatility. A typical OA concentration is of the order 1 μg m^{-3} (a mass fraction of 1 ppbm) and, if the molar weight of the SOA molecules averages 200 g $mole^{-1}$, the mole fraction of OA is roughly 100 ppt. If OA consisted of a single, pure organic compound and it had a saturation vapor pressure of 10^{-7} Torr (1.3×10^{-5} Pa), that compound would be 50% in the gas phase and 50% in the condensed phase at equilibrium under ambient conditions. That is a good definition of a semi-volatile constituent. Compounds with this saturation vapor pressure (over a sub-cooled liquid state) include pentacosane ($C_{25}H_{52}$, the canonical paraffin) and glucose. Those are not molecules one normally considers "semi volatile"; it is thus reasonable to expect standard intuition to be off target when considering organic aerosol. Of course, OA particles are *not* pure but rather contain thousands of different molecules, so mixing thermodynamics plays an important role as well. Furthermore, paraffin and glucose are notably viscous, so it is not necessarily surprising that viscosity effects may be important to OA behavior.

2.1 Phase Partitioning Thermodynamics

The thermodynamics of semi-volatile phase partitioning for atmospheric OA mixtures has been extensively treated in the literature [17, 18, 39, 40] and will only briefly be reviewed here. We express the effective saturation concentration $\left(C_{\mathrm{i}}^{*}\right)$ of an organic compound by converting its saturation vapor pressure into mass concentration units and multiplying by the appropriate activity coefficient for the organic mixture (this is the inverse of the partitioning coefficient used in some formulations: $K_{\mathrm{p,i}} = 1/C_{\mathrm{i}}^{*}$). The general effect of a solution is to lower the equilibrium partial pressure of a species from the equilibrium vapor pressure of the pure species; if the fractional reduction in the partial pressure (the activity) is equal to the fraction in the condensed phase, the solution is ideal and Raoult's law applies. One simplifying assumption is to treat the system as a "pseudo-ideal" solution [23] in which the activity coefficients of individual compounds remain more or less constant over ambient conditions, in which case C_{i}^{*} for a given compound will remain constant as well.

The fundamental property of interest is the equilibrium fraction ξ_{i} of a compound in the condensed phase (vs the total in the condensed and vapor phases). With a total concentration of condensed-phase solute (often assumed to be the total concentration of organic aerosol, C_{OA}), this is given very simply by

$$\xi_{\mathrm{i}} = \left(1 + C_{\mathrm{i}}^{*}/C_{\mathrm{OA}}\right)^{-1}. \tag{1}$$

This is a straightforward equation. It is evident that when the total OA concentration equals the saturation concentration of a constituent $\left(C_{\mathrm{i}}^{*} = C_{\mathrm{OA}}\right)$, that constituent will be 50% in the condensed phase at equilibrium ($\xi_{\mathrm{i}} = 0.5$).

Furthermore, a constituent with $C_i^* = 0.1\ C_{OA}$ will be ~90% in the condensed phase while a constituent with $C_i^* = 10\ C_{OA}$ will be only ~10% in the condensed phase. There is thus a fairly narrow range of (extremely low) volatilities spanning approximately a factor of 100 in C^*, centered around C_{OA}, where a compound will be "semi volatile." Furthermore, this range varies with the aerosol loading – at high C_{OA} of perhaps 100 μg m^{-3} found in very polluted cities (or source-dominated locations such as highway tunnels), the whole range of semi-volatiles will be shifted by a factor of 100 toward higher volatility. Also, experiments with significantly higher aerosol concentrations may not have phase partitioning consistent with the atmosphere. Until quite recently aerosol chamber experiments were performed with hundreds to thousands of micrograms per cubic meter of aerosol, resulting in phase partitioning very different from ambient conditions. Emissions measurements are still routinely performed at these unrealistic conditions.

There are at least three separate ways of treating partitioning for practical application to atmospheric aerosol. One is to run a full thermodynamic model containing an ensemble of specific molecules, while the other two are empirical.

2.1.1 Explicit Methods

Explicit methods seek to treat chemistry and thermodynamics with molecular detail, either including as complete a set of compounds as possible [41] or employing a reduced set of surrogate compounds to represent the full array of atmospheric compounds [21]. In either case the thermodynamics for this model system are treated as fully as possible, with individual vapor pressures and activity coefficients for the mixture calculated using one of several thermodynamic schemes [42–45]. A major challenge for this approach is the fact that the molecular composition of the vast majority of the OA mass is not known. However, when OA composition is known or if it can be predicted, they do allow one to assess as completely as possible the consistency of available data.

Recent studies on SOA derived from α-pinene are a good illustration of the explicit methods. Simulations of α-pinene ozonolysis using detailed chemistry from the Master Chemical Mechanism reproduce both SOA mass yields and the volatility distribution derived from chamber studies with good fidelity [46], though an earlier simulation using similar MCM chemistry but different vapor pressure estimation methods under-predicted SOA mass yields at low loading ($C_{OA} < 10$ μg m^{-3}) [47]. A tailored α-pinene oxidation mechanism also performs well in comparison with chamber experiments [48]. A generative mechanism (GECKO-A) applied to α-pinene photo-oxidation generally over-predicts SOA formation, especially under low-NO_x conditions [49]. None of those simulations modeled additional condensed-phase oligomerization chemistry. While the model-measurement intercomparisons were in general good, the dual uncertainties of the chemical mechanisms and vapor pressure estimation greatly complicated substantive intercomparisons, even when additional measurements such as oxidation state of the SOA were included [46, 49].

2.1.2 Empirical Methods

Empirical methods are based on fits of partitioning data (generally chamber observations) to identify a set of pseudo-compounds with different abundances, which can then be used to simulate the gas-particle partitioning of OA. A major challenge with this approach is whether the properties of these pseudo-compounds are constant as one extrapolates away from the conditions under which the experiment was conducted. To help minimize these errors, it is critical to condition the partitioning experiments over as much atmospherically relevant space as possible.

N-Product Models

The most widely used empirical method is the "Odum two-product model" used to interpret many chamber experiments and implemented widely in air-quality models [23, 50]. When chamber SOA formation data are fitted to a two-product model, the output parameters are two mass yield parameters and two partitioning coefficients ($K_{\mathrm{p,i}} = 1/C_{\mathrm{i}}^{*}$), giving a total of four free parameters. The two pseudo-species are not typically associated with any particular molecular products but rather regarded as completely empirical objects. In general they split into a "low-volatility" and a "high-volatility" product. One issue is that the recovered C^{*} values are highly dependent on the experimental dataset. The C^{*} values recovered from data fitting often coincide approximately with the range of measured C_{OA} values in the data, so the volatility of the two pseudo products depends on the concentration range of the experiments [51]. As an example, the C^{*} value commonly used for isoprene SOA is approximately 1 μg m^{-3} [52], while the "low-volatility" C^{*} value used until recently for α-pinene SOA was higher, at 15 μg m^{-3} [53, 54]. It would be surprising if SOA derived from isoprene (with five carbons) were less volatile than SOA derived from α-pinene (with ten carbons); however, because isoprene SOA experiments produce much less SOA than α-pinene SOA experiments, the empirically derived product volatilities are skewed. This can have unexpected consequences when the two systems are mixed in a model simulation, where the presence of isoprene SOA will "seed" more volatile α-pinene SOA formation. Reality is more likely to be the opposite of this.

Some of the deficiencies of the empirical two-product model can be eliminated by adding information to a multiple product model. One solution is to map products from chamber experiments onto a "carbon-number–polarity grid" based not only on the empirically observed SOA mass but also expected product properties [55]. Chemical evolution could be described on the grid, enabling a sensible description of aging.

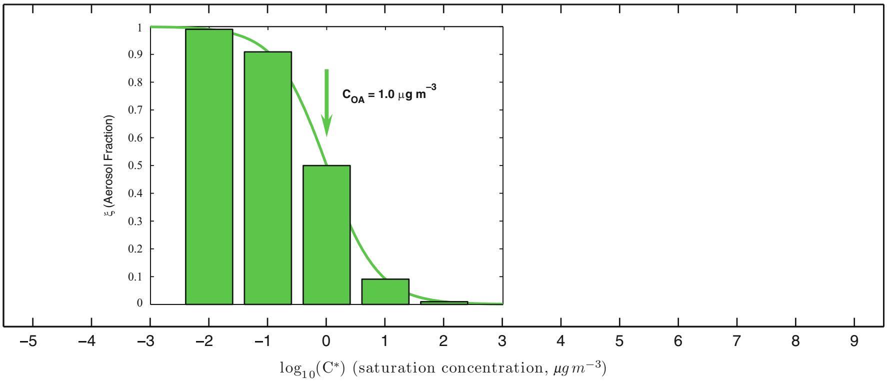

Fig. 1 Partitioning behavior of organics for 1 μg m^{-3} of total organic aerosol (C_{OA}), shown as the fraction in the condensed phase (ξ, height of *bars* and *curve*) vs saturation concentration (C^*)

Volatility Basis Set

Another empirical approach is known as the "Volatility Basis Set" (VBS). Like the two-product model, the VBS is empirical. However, the pseudo-product volatilities are fixed over a wide range, with C^* values typically separated by a single order of magnitude at 300 K [40]. An example is shown in Fig. 1. In a VBS fit the free parameters correspond to the different total concentrations (in any phase) in each volatility "bin" (each pseudo product). Thus, a VBS fit to SOA data with C^* bins at 1, 10, 100, and 1,000 μg m^{-3} has the same number of formal degrees of freedom as a two-product model, but there is a crucial difference. Because the VBS C^* values are fixed, the overall partitioning function (Eq. 1) is only sensitive to the volatility of a given bin when C_{OA} is within about a single order of magnitude of the C^* value for that bin. The VBS parameters are thus relatively robust and independent of each other (there is covariance among adjacent bins, however, and so data can often have many equally good fits where material is divided differently among neighboring bins [56]). VBS parameters can only be fitted to data over slightly more than the range of C_{OA} values in a dataset – the extremes at lower or higher volatility must be constrained by other means, such as an overall carbon balance. With those constraints, a nine-bin VBS is often employed with C^* ranging from 0.01 μg m^{-3} to 10^6 μg m^{-3} [38]. This spans the full range of fully condensed organics, semi-volatile vapors, and "intermediate volatility" species and permits a good carbon mass balance. Though this requires nine species for transport in a model, if all organics form a pseudo-ideal solution the VBS fits from different OA sources can easily be combined to predict overall partitioning for a mixture without the unexpected consequences sometimes emerging from the two-product model.

Non-ideality

A downside of the empirical approaches is they give little insight into non-ideal behavior of complex mixtures, including mixing effects of different organics (their activity coefficients), interaction with water, and interaction with inorganic constituents including salts and elemental carbon. These latter two types of interactions typically involve significant extrapolation away from the conditions of the experiments used to derive the fits. Unfortunately, there are very few direct measurements of activity coefficients for relevant organic molecules over relevant organic mixtures. It seems reasonable to expect seemingly similar OA, such as SOA derived from different precursors, to interact in a more or less ideal fashion, and indeed isotopic labeling experiments have confirmed this [57, 58]. However, mixing of less similar organics, such as relatively non-polar POA and more polar SOA, is less clear. Some experiments using non-polar organic "seeds" show little enhancement in SOA formation over experiments employing inorganic seeds [59], while other experiments directly observing mixing of SOA and POA by tracking the evolution of different size modes using size-resolved mass spectrometry show more nuanced behavior, with rapid mixing of semi-volatile POA into SOA seeds in some cases but not in others [60].

While methods based on explicit surrogate molecules (or complete enumeration of the organic mixture) can rely on calculated activity coefficients, the empirical methods must rely on approximations. In two-product SOA schemes one approach is to assume that generally similar classes of species mix with each other ideally (for example all SOA pseudo-products), but to permit either ideal mixing or complete phase separation of less similar constituents (for example SOA with POA) [23]. More generally, the empirical methods contain very little information about the molecular structure of OA constituents as they are based only on observed gas-particle partitioning and total mass concentrations. This complicates calculations not only of activity coefficients but also of important properties like the organic mass to organic carbon ratio (OM:OC) or the closely related oxygen to carbon ratio (O:C). Of course, composition information can be added based on additional observations, as with the carbon-number–polarity grid described above [61]. However, with the one-dimensional VBS there is an intrinsic problem: compounds with similar volatility can be very different chemically. For example, two compounds with a (sub-cooled liquid) saturation concentration near 10 μg m^{-3} are tricosane ($C_{23}H_{48}$) and levoglucosan ($C_6H_{10}O_5$). Each are important in the atmosphere – tricosane is a constituent of lubricating oil [9] while levoglucosan is an important tracer for wood burning because it is a cellulose pyrolysis product [62] – but it is not surprising that lumping both into an identical bin in the 1D-VBS could obscure critical differences in their behavior.

An important issue to consider is the consequence of non-ideality. Interactions that enhance partitioning to the particle phase are important because they increase aerosol concentrations and also often shield organics from the gas-phase oxidation discussed below. However, interactions that increase volatility will drive compounds into the gas phase where they will likely be oxidized quickly. In many cases the reaction products will return to the condensed phase, though on different particles and in a higher oxidation state. It is thus essential that one considers phase partitioning and aging together, and also that the coupled issues be considered jointly when developing simplified parameterizations for complex chemical transport models.

Two-Dimensional Volatility Space

A two-dimensional version of the VBS addresses the issues just described, including non-ideality and the substantial differences in species contained in a single bin of the 1D-VBS [63, 64]. In addition, the two-dimensional volatility space (2D-VBS) enables more realistic treatment of aging chemistry and important properties such as hygroscopicity. The second dimension is formally the average oxidation state of carbon (OS_C) described in Kroll et al. [65], which is related to the oxygen to carbon ratio (for "normally" bonded molecules, $OS_C = 2$ O:C – *H:C*). Figure 2a shows the average molecular composition (carbon number, n_C; hydrogen number n_H; oxygen number n_O) in this space and also the approximate O:C for typical ambient aerosol composition [66]. Also shown are the measured saturation concentrations and OS_C for tricosane and levoglucosan. This shows that the approximate formulae given by the contours are not far off from observations, that these seemingly non-volatile species are in fact quite volatile by atmospheric standards, and that in the 2D space these quite different species are well separated even though their volatilities are nearly identical.

The *x* axis in the 2D-VBS is formally the pure-component saturation concentration C^o rather than the effective saturation concentration C^*, which includes the activity coefficient: $C^* = \gamma C^o$. A simplifying assumption in the 2D-VBS is that the activity coefficient is a function of the average O:C of the OA as well as the properties of the individual organic solute [63]. Figure 2b shows γ as an example for a case where the O:C of the bulk OA is 0.5 (typical of fairly fresh oxidized organic aerosol (OOA) in an urban setting [67]). In this case the contours are for different pseudo species (or bins) in the 2D-VBS. For example, a species with a C^o of 1 μg m^{-3} and an O:C of 0.1 would have $\gamma = 10$ (the last contour shown), meaning $C^* = 10$ μg m^{-3} for that particular mixture. The notable thing in Fig. 2b is that the predicted activity coefficients are mostly very close to 1, with the exception of very reduced material in the paraffin range typically associated with POA emissions. This confirms that most SOA species (with elevated O:C) will tend to form a nearly ideal solution with each other and only the semi-volatile POA species will tend to either phase separate into a distinct condensed phase or else have a *higher* partial pressure and thus partition toward the gas phase.

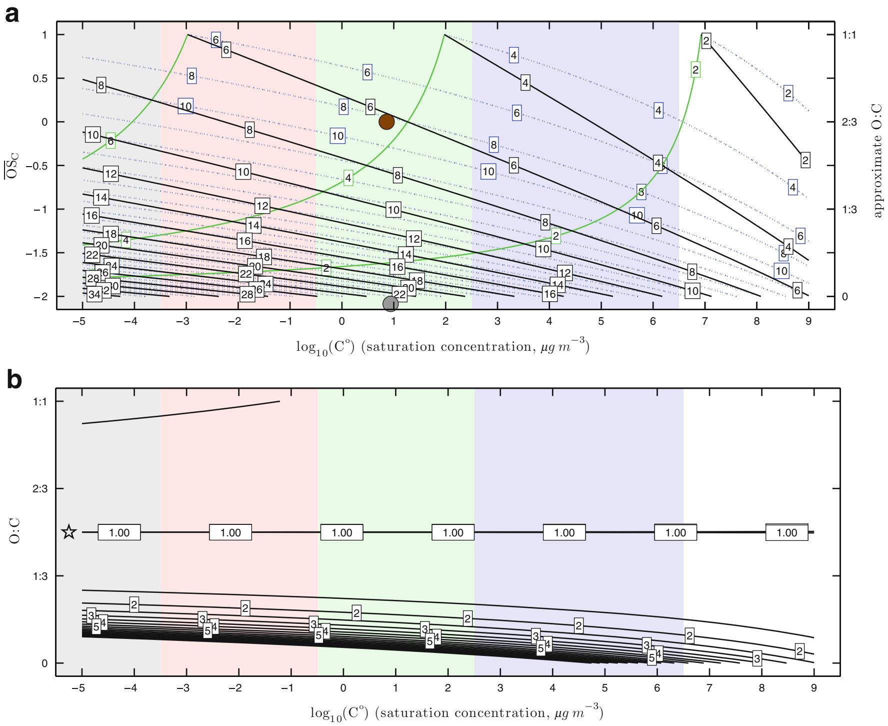

Fig. 2 (**a**) Organic aerosol composition in 2D space defined by pure component saturation concentration (C^o) and average carbon oxidation state (OS_C). *Solid black lines* extending from lower left to upper right are average carbon number (n_C). *Solid green curves* bending from top to lower left are average oxygen number (n_O). *Dashed blue curves* bending from bottom to upper left are average hydrogen number (n_H). Measured saturation concentrations for tricosane ($C_{23}H_{48}$, *gray circle*) and levoglucosan ($C_6H_{10}O_5$, *brown circle*) are shown as well. Both are semi volatile under ambient conditions. (**b**) Activity coefficients of organics in an organic solution with an average O:C = 0.5 (typical of fresh SOA or urban conditions). Contours are spaced by 0.5 and extend to 10.0. Values in the lower left of the space (occupied by compounds typically constituting POA) are much larger than 10.0

Temperature Dependence

The temperature dependence of saturation concentrations can be approximated to first order by an Arrhenius type equation resembling the Clausius Clapeyron equation [40, 68]:

$$C^o(T) = C^o(300)\exp\left[\Delta H_{\mathrm{vap}}/R(1/300 - 1/T)\right]. \tag{2}$$

In the VBS formalism the effect of changing temperature is to shift the C^* (or C^o) values of the bins. The bins themselves shift with temperature – one does not repartition material from one bin to another. This is straightforward [40, 69]. The exact ΔH_{vap} for organic compounds remain a topic of some debate, but for a ΔH_{vap} near 100 kJ mole^{-1}, a temperature change of 20 K results in a one-decade shift in a volatility bin.

2.2 Dynamics of Condensation and Evaporation

The equilibrium thermodynamics described above applies to all systems, but a key question is whether atmospheric systems actually reach that equilibrium. Furthermore, equilibrium phase partitioning says little about what size particles organic compounds end up on. The dynamics of organic condensation and evaporation have recently gained renewed attention for several reasons. First, it is clear that in many environments organic condensation plays a critical role in the growth of freshly nucleated particles up to diameters of 100 nm or so [70–75], where they can influence cloud physics by acting as cloud condensation nuclei. Because the timescale for growth of these ultrafine particles is similar to the production and loss timescales of the condensable vapors, a dynamic treatment is required. Second, there is also growing evidence that many particles containing OA may be in a highly viscous (glassy) state [32–34]. For particle growth, the *net* condensation rate of organics to particles is critical because that controls the growth rate. For glassy particles, diffusion limitations within particles may be rate limiting in condensation and growth, potentially preventing semi-volatile organics from reaching equilibrium on atmospherically relevant timescales [31]. In-particle diffusion limitations could cause apparent mass accommodation coefficients well below unity.

The VBS provides a convenient framework for organic dynamics in addition to equilibrium partitioning because equilibrium is a balance between condensation (the molecular flux from the gas to the particle phase) and evaporation (the molecular flux from the particle phase to the gas). The difference between the vapor concentrations at the particle surface and far away from it serves as a driving force for *net* condensation or evaporation. Because the particle surface is usually assumed to be in equilibrium with the gas phase adjacent to it, evaporation depends explicitly on volatility. Condensation on the other hand depends only on the collision rate of molecules with the surface and so it is first order independent of volatility. The volatility of organic compounds thus affects the aerosol growth dynamics specifically through its influence on the evaporation term in the driving force for mass transport.

It can be shown that the intrinsic growth or evaporation rate associated with a given organic volatility is given by $v_D C_i^*$ where the characteristic velocity v_D is 226 nm h^{-1}/(μg m^{-3}) [75]. This is modified by three important terms – the mass accommodation coefficient, α, the surface-energy (Kelvin) term for particles smaller than 50 nm or so, and the Fuchs term for gas-phase diffusion limitations in the boundary layer around a particle for particles *larger* than 50 nm or so (with Knudsen numbers $Kn \leq 1$). Barring other limitations, the evaporation rate (in nanometers per hour) for a pure particle with a gas-phase concentration C_i^{vap} held at 0 is thus given by

$$\mathrm{d}d_\mathrm{p}/\mathrm{d}t = F\left(d_\mathrm{p}\right)K\left(d_\mathrm{p}\right)C_\mathrm{i}^{*}\alpha_\mathrm{i}\nu_\mathrm{D}. \tag{3}$$

This corresponds to a volume evaporation rate from a spherical particle of

$$\mathrm{d}V/\mathrm{d}t = {}^1\!/_2\pi d_\mathrm{p}^2 F\left(d_\mathrm{p}\right)K\left(d_\mathrm{p}\right)C_\mathrm{i}^{*}\alpha_\mathrm{i}\nu_\mathrm{D}. \tag{4}$$

Given a volume $V = 1/6\pi d_\mathrm{p}^3$, we can define a timescale for mass transfer via condensation or evaporation from a particle as $\tau_\mathrm{e} = V/(\mathrm{d}V/\mathrm{d}t)$, or

$$\tau_\mathrm{e} = \left(3F\left(d_\mathrm{p}\right)K\left(d_\mathrm{p}\right)C_\mathrm{i}^{*}\alpha_\mathrm{i}\nu_\mathrm{D}\right)^{-1}d_\mathrm{p}. \tag{5}$$

This timescale for a given species is independent of the fraction of that species present in an ideal organic mixture, but it is based on the limit of little net diameter change (evaporation of a pure particle will be quicker because the expression must be integrated down to zero volume). The timescale as a function of d_0 is shown in Fig. 3 for unit mass accommodation and pure particles made up of constituents with different C^* values. The central bold curve is for $C^* = 1\ \mu\mathrm{g\ m}^{-3}$. Actual equilibration timescales will differ from this characteristic evaporation timescale; the exact timescale for equilibration of compounds in particles containing organic mixtures will depend on the extent of growth or evaporation required for a mixed particle to reach equilibrium. This in turn depends on the number concentration of particles because that dictates the total mass exchange between condensed and vapor phases, and for low volatility species equilibration timescales are often controlled by the condensational timescale, which can be faster than the evaporation timescale [76, 77]. Regardless, the intrinsic evaporation timescale for $C^* = 1\ \mu\mathrm{g\ m}^{-3}$ organics in 200 nm diameter particles is very nearly 1 h. Timescales for more or less volatile compounds can be found simply by multiplying these values by C^* in $\mu\mathrm{g\ m}^{-3}$, as shown by the parallel curves for different C^* bins. For example, in a typical SOA formation experiment from α-pinene in which 100–1,000 $\mu\mathrm{g\ m}^{-3}$ of SOA is formed, both VBS and two-product fits of product volatilities suggest that much of the SOA consists of species with volatilities also in the 100–1,000 $\mu\mathrm{g\ m}^{-3}$ range. One would thus expect these SOA particles to evaporate substantially in 30 s to 6 min if the gas phase were forced to remain free of vapors.

There are at least three reasons why an evaporation timescale could be *longer* than the intrinsic value shown in Fig. 3. First, the actual mass accommodation coefficient α for the compound could be less than 1 [78, 79]. Mass accommodation is defined as the fraction of vapor collisions with the surface of a particle that wind up adsorbed onto that surface as opposed to more or less immediately rebounding from the surface. There is some debate for light molecules such as water as to whether α must be unity or whether it may be as low as 0.04 [80–84], and the average α for CO_2 from perfluoronated polyether (PFPE) is also approximately 0.5 [85]. Values of

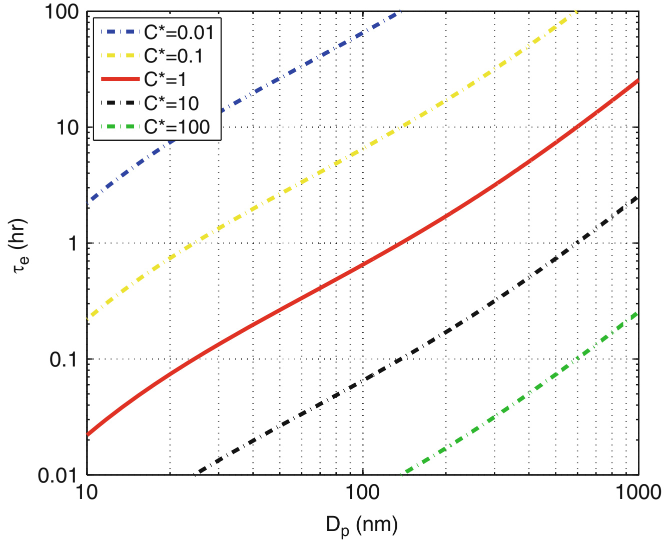

Fig. 3 Characteristic evaporation timescales for organics vs particle diameter for a series of volatilities (C*) defined by contours. Organics with $C^* = 1\ \mu g\ m^{-3}$ in a 200-nm particle will evaporate in approximately 1 h if mass accommodation is perfect and diffusion within the particle is more rapid than 1 h

$0.1 \leq \alpha \leq 1$ seem plausible and have been reported for pure systems [86]. Lower values seem unlikely. However, even the meaning of α at a molecular level is not firmly established and so non-unit accommodation coefficients must remain under consideration. Regardless of the exact value, at any given time the accommodation and evaporation coefficients for a molecule must be the same, or else the physical process responsible for changing α would instead really be changing the C^* value itself.

The second possibility for slower evaporation is diffusion limitations within the particle itself, or possibly slow annealing of a particle to its equilibrium morphology (as in Ostwald's ripening). In this case the surface composition would not reflect the average composition of the particle. Glassy particles typify this possibility. The timescale for diffusive mixing of a constituent in a spherical particle is $\tau_m = d_p{}^2/(4\pi^2 \times 3{,}600\ D)$ [87], where D in $cm^2\ s^{-1}$ is the diffusion constant of that constituent in the particle, and τ_m is again expressed in h. Just as we use $1\ \mu g\ m^{-3}$ as a characteristic volatility, we shall use 200 nm as a characteristic diameter ($200\ nm^2$ is $4 \times 10^{-10}\ cm^2$). Given these constraints, a 1-h or greater mixing timescale in a 200 nm diameter particle requires a diffusion constant (for the diffusing constituent in the mixture) of $D \leq 10^{-14}\ cm^2\ s^{-1}$. Alternately, it has been suggested that a thin coating of very viscous material on particles may inhibit organic mass transfer of higher volatility molecules to the particle surface, thus slowing or preventing evaporation [31]. Assuming a coating thickness of 10 nm, the diffusion coefficient of the evaporating molecules in this crust would have to be $D \leq 3 \times 10^{-16}\ cm^2\ s^{-1}$

for the timescale to exceed 1 h. These are very low numbers, and no direct measurements of molecules/mixtures with such low binary diffusivities exist. Koop et al. [34] report that the primary predictor for the glass transition temperature in organics (indicative of $D \leq 10^{-20}\,\mathrm{cm}^2\,\mathrm{s}^{-1}$) is the molecular weight, followed by the degree of oxygenation (i.e., molecular polarity). Compounds with glass transition temperatures of 300 K are tricarboxylic acids with molecular weights of order 200 g/mole. Extension to $D(T)$ for mixtures containing much less polar constituents remains unclear.

A third factor potentially influencing evaporation timescales of organic compounds is the presence of weakly bound oligomeric species or organic salts with dissociation lifetimes greater than the evaporation timescale. Even a weakly bound species, with a binding energy of 100 kJ mole^{-1} and a unimolecular dissociation A factor of 10^{14} s^{-1}, would have a 1-h dissociation timescale at 300 K. Alone among these confounding factors, thermal decomposition can easily lead to an evaporation timescale that is independent of particle size; if the decomposition itself is the rate-limiting step for particle evaporation, the timescale will be fixed by the chemistry and not a mass-transfer limitation.

3 Evidence for Volatility in Atmospheric Aerosol

There is compelling evidence that a significant fraction of OA constituents are semi-volatile, with dynamic gas-particle partitioning under atmospheric conditions. However, the evidence also suggests that volatility is greatest near source regions, where aerosol is "fresh" [69, 88]. This is consistent with the hypothesis that chemical aging generally reduces, or really "resolves" volatility, driving semi-volatile species either toward relatively stable lower volatility products or toward highly volatile, highly oxidized small organic molecules (and ultimately CO_2).

3.1 Volatility of Primary Organic Aerosol

Despite the historical tendency of models to represent POA as a non-volatile mixture, there is longstanding and compelling evidence that POA emissions are substantially semi-volatile. The evidence comes in two major forms. First, both volatility-based chromatography and molecular elucidation of emissions profiles for various sources show clearly that most POA emissions span a wide range of C^* values and that most of those are $\gg$1 μg m^{-3} [89, 90]. This is often simply a consequence of the properties of the parent materials for the emissions, such as lubricating oil. Second, when the gas-particle equilibrium is perturbed, either via isothermal dilution or via heating, POA particles shrink.

The second characteristic of primary organic emissions is that they tend to be relatively reduced. Using the average carbon oxidation state as a measure [65], most

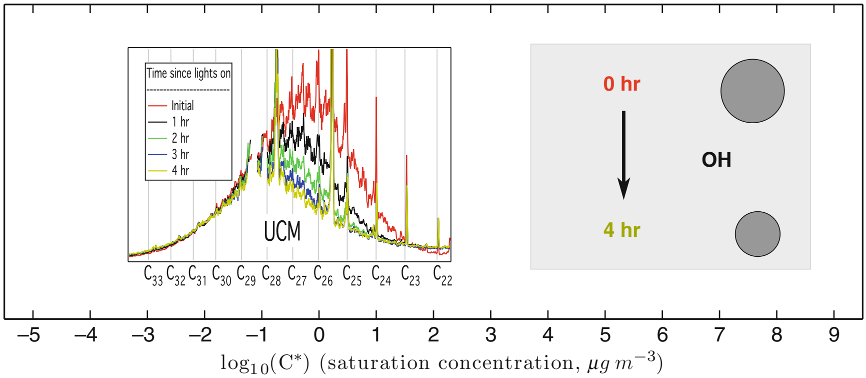

Fig. 4 Oxidation of a motor oil mixture by OH radicals in a smog chamber, followed by thermal desorption gas chromatograms (TAG) taken every hour. Carbon numbers in the chromatogram are registered to typical saturation concentrations. More volatile organics ($n_C < 28$) are removed more rapidly, indicating that gas-phase oxidation dominates the removal

but not all primary organic emissions have an $OS_C \leq -1.5$. This has significant consequences for aging chemistry, but in practical terms it also means that the emissions are relatively nonpolar and thus relatively easy to elute from standard gas-chromatograph columns.

As just one example of volatility separation, in Fig. 4 we show chromatograms of nebulized motor oil particles from an experiment in the CMU smog chamber using a thermal-desorption aerosol gas-chromatography (TAG) system [91], registered in the 1D-VBS. The figure shows two things. First, the red trace shows the initial chromatogram from oil droplets at $C_{OA} \sim 10$ μg m^{-3}. Only hydrocarbons with $n_C \geq 23$ appear in the condensed phase because the more volatile constituents evaporate once the droplets are diluted to low concentrations in the chamber. Second, the experiment involved subsequent exposure to OH radicals, and the series of colored traces show chromatograms of non-polar material for each hour [92, 93]. Clearly, the more volatile fraction of the motor oil decayed much more rapidly than the less volatile fraction. The experiments showed simultaneous buildup of secondary oxidized organics on the particles [93]. This is consistent with gas-phase oxidation of vapors from that volatile fraction causing evaporation to compensate for the gas-phase loss, while heterogeneous oxidation of the less volatile constituents via OH uptake is evidently much slower [92].

Isothermal dilution consistently reveals that POA particles are semi-volatile [90]. Specifically, when POA samples are diluted, the particles shrink. They shrink because the gas-phase dilution lowers the partial pressure of vapors over the particles, and the particles respond to this perturbation by evaporating to raise the partial pressure of those vapors back to equilibrium. Analyses of POA dilution data suggest that a large fraction of the POA mass falls in the 1–1,000 μg m^{-3} range [56, 94].

Evaporation upon heating can complement isothermal dilution. Most POA species are saturated and so are relatively inert and thermally stable; heating is thus unlikely to induce chemistry. Consequently, shrinking on heating in a thermodenuder is unambiguous evidence that the condensed-phase species in a POA particle are semi-volatile. An extra uncertainty associated with thermodenuders is the vaporization enthalpy of the organics [68]; however, as discussed above, a temperature change of 20 K corresponds roughly to an order of magnitude change in C^* (also a change in n_C of 2 corresponds to an order of magnitude change in C^*). Most POA emissions evaporate quite readily in a thermodenuder [56]. For example, lubricating oil such as that shown in Fig. 4 evaporates almost completely when heated by 40 K, and one can see that a shift in the (unreacted) mode from $n_C = 26.5$ to 30.5 should indeed correspond by substantial evaporation.

Several studies of primary particles near sources such as roadways [95] and fires [96] have also established that primary particles tend to shrink as they are isothermally diluted during dispersion downwind of a concentrated source [97, 98].

The bottom line is that emissions from (typically high-temperature) POA sources such as internal combustion engines, wood burning, and food preparation are all characterized by constituents with a broad range of volatilities, a large fraction of which have $C^* > 1\ \mu g\ m^{-3}$ [90]. Consequently, most of these emissions, even those with vapor pressures many orders of magnitude lower than traditional "volatile organic carbon," will be in the gas phase very soon after emission (in seconds to minutes). The subsequent gas-phase chemistry of those vapors is thus one form of aging to consider in organic-aerosol evolution.

3.2 Volatility of Secondary Organic Aerosol

Somewhat ironically given the history of SOA and POA, SOA volatility is a more complicated topic than POA volatility. The principal reason is that SOA species are by definition products of reactions in the atmosphere, and many product compounds are themselves highly reactive. In addition, more oxidized organic species tend to be more polar than their reduced precursors and thus more difficult to sample using separation techniques. Furthermore, the added functionality associated with oxygenation opens up a vast space of potential chemical species, rendering complete speciation of a sample practically impossible [65]. In spite of this, there is every reason to believe that most SOA (especially "fresh" SOA) has a significant amount of semi-volatile mass.

Because of their comparatively large flux to the atmosphere [99], terpenes have long been a major focus of SOA-formation experiments [15]. Significant effort has been expended on speciating SOA, and while the complete mass has not been elucidated, many important product species have been identified [100, 101]. For example, with α-pinene SOA many C_{10} products have been identified, and their C^* values range from roughly 1 to > 1,000 $\mu g\ m^{-3}$ [46, 49]. Recently, two-dimensional chromatography has been employed to combine volatility and polarity separation in a manner highly complementary to the 2D-VBS described above. 2D-GC can be mapped onto the 2D-VBS and, for example, a substantial amount of the eluted material from SOA formed via the longifolene + ozone reaction falls in the 0.1–10 μg m^{-3} range, with O:C varying systematically from about 0.25 at the low C^* end to about 0.1 at the high C^* end [102]. Longifolene is a sesquiterpene ($C_{15}H_{24}$), and the observed C^*–O:C range is consistent with the range expected for product molecules with 12–15 carbons seen in Fig. 1a.

Less volatile compounds have been observed from terpene-ozone SOA as well, including C_{20} and larger "oligomers" [103–105] and very low volatility organosulfates [106]. It remains unclear what fraction of the SOA mass is comprised of these less volatile species, but estimates range from 1/3 to 1/2 [105]. It is also not clear whether the majority of oligomers are formed irreversibly or whether they are in equilibrium with monomer species [107]. What is clear is that a substantial fraction of the SOA mass consists of semi-volatile monomeric species, and one thus expects phase partitioning to play a major role in their behavior.

Indeed, absorptive partitioning theory [18] played a critical role in the interpretation of SOA chamber data, making sense of a confusing disarray of mass yield data [17]. Specifically, partitioning theory explains the general tendency for mass yields to increase with increasing total OA concentrations. In Fig. 5 we show mass yield data for the α-pinene + ozone reaction along with a representation of the rising yields with increasing C_{OA}. In this figure C_{OA} (in micrograms per cubic meter) is plotted on the same axis as C^* (also in micrograms per cubic meter). The concentration range over which mass yields rise sharply is the concentration range where the bulk of the products lie – in this case $C^* \geq 1$ μg m^{-3}. An extremely important caveat is that this partitioning analysis is only valid if the overall product distribution (including the condensed and vapor phases) remains constant during a chamber experiment, so that only thermodynamics and not chemical aging governs the amount of material that partitions into the particle phase (in other words, C_{OA} responds to the amount of identical products being produced and not to changes in the product and volatility distribution over the course of a reaction). The very small mass yields at very low C_{OA} pose a challenge to quantitative treatment of the oligomerization reactions described above, as even at fairly low C_{OA} particles in chamber experiments are quite stable, maintaining a constant diameter over many hours [101] and thus showing no clear evidence (no increase of SOA mass) of any slow chemical reactions that might slowly alter the volatility distribution.

To be truly consistent with partitioning theory, particles must also shrink upon dilution, much like POA described above. Different experiments have confirmed that α-pinene + ozone SOA particles do evaporate upon dilution, but not in the minute or so suggested by the volatility distribution in Fig. 5 and the timescales in Fig. 3. Rather, particles relax back to equilibrium after dilution over hours [31, 108], though they do eventually reach the size predicted from equilibrium partitioning theory [108]. This delay is consistent with some phenomenon slowing evaporation by at least a factor of 100. Potential causes for this delay include dissociation of weakly bound oligomers [108] or slowed diffusion in the particles themselves

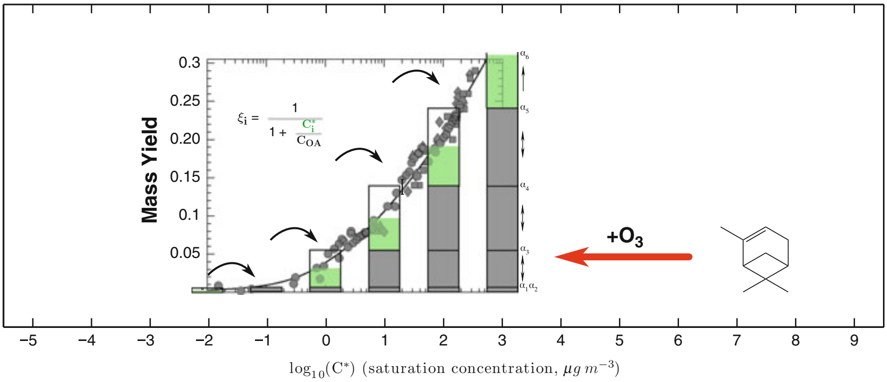

Fig. 5 SOA mass yields from α-pinene ozonolysis vs total SOA mass (C_{OA}). Increasing mass fractions with increasing C_{OA} are consistent with progressive partitioning of more volatile products at higher loadings, as shown

[31, 108]. A recent study [31] reports that size selected α-pinene + ozone SOA particles at $d_p = 160$ and 250 nm showed nearly identical evaporation behavior, whereas the timescales in Fig. 3 are a factor of 2 different. That is consistent with a dissociation timescale being rate limiting as opposed to pure evaporation.

A final element in the evidence supporting a substantially semi-volatile nature for most "fresh" SOA comes from thermodenuders. As with POA, SOA formed in smog chambers evaporates quite readily in thermodenuders [109–113]. Quantitative analysis (inverting thermodenuder data to find a volatility distribution) is difficult because of several confounding factors. These include uncertainties in ΔH^{vap} as well as the mass accommodation coefficient [69, 77]. An extra cause of concern with SOA, unlike POA, is the potential for the SOA to change chemically when it is heated [68]. However, with significant evaporation of chamber-derived "fresh" SOA mass after only 40 K of heating, thermodenuder data are certainly consistent with a substantial fraction of the SOA mass from chamber experiments being semi volatile [110, 114].

Ambient SOA, or at least the highly-oxygenated OOA, generally loses much less mass in thermodenuders [29, 69, 115] than fresh SOA, suggesting that it is much less volatile. Inversions using a VBS framework find a very broad distribution of C^* values for OOA constituents, suggesting (along with the high degree of oxidation) that OOA has undergone substantial oxidative aging in the atmosphere [64, 69].

3.2.1 Do OA Particles Form Mixtures?

In order for mixing thermodynamics to apply, an OA particle must actually be mixed. There are compelling reasons to believe this is so but also some reasons to question whether the mixing is complete. This question really splits into two questions: is the *equilibrium* for OA constituents a uniform mixture and, if so, do ambient particles relax to that equilibrium more rapidly than they are transported or lost?

There is little doubt that most organic compounds in ambient particles exist in some form of mixture, simply because the particles are composed of an enormous number of different molecules. In the most extreme cases a single constituent can make up as much as 10% of some ambient particles (for example levoglucosan near some fire plumes or certain isoprene oligoesters in very isoprene-rich environments) [116, 117]. However, in most cases the most abundant identified constituent in OA samples comprises less than 1% of the total OA mass. Consequently most organic molecules in most particles are far more likely to be solvated by and interacting with many different molecules with a variety of carbon chain lengths, branching structures, and numbers and types of functional groups. This is one reason why crystallization seems highly unlikely for most particles and consequently why the mixing thermodynamics are developed for amorphous mixtures (thus employing the sub-cooled liquid vapor pressure as the starting point for partial-pressure calculations) [18]. This also provides information on experimental design, especially relating to organic "seeds" for SOA formation that might promote condensation via absorptive partitioning. High fractions of any individual seed species will enhance the probability that a separate (potentially crystalline) "seed phase" will form in an experiment, while more realistic seed mixtures will be less vulnerable to such phase separation.

A second factor favoring mixtures is that most OA constituents arrive in a particle via condensation. The organic condensation rate in the boundary layer under many conditions is roughly 1–10 nm h^{-1} [73]. Near sources there will be (sometimes concurrent) evaporation and condensation of POA species, and both near and far from sources there will be condensation of oxidized secondary molecules as well as uptake of oxidants. Furthermore, in many cases important inorganic species such as sulfuric acid, nitric acid, and ammonia are condensing (and in the latter two cases evaporating) from particles simultaneously. Perhaps most importantly, as relative humidity (RH) varies, the activity of water in a particle will vary as well. Above about 90% RH, more than half of the volume of most particles will be water, and this water will form an extremely high ionic strength aqueous phase incorporating at least some of the more soluble organic molecules (and even the "hydrophobic" residual organic phase may include significant water). Under many circumstances air parcels move vertically through the boundary layer in minutes, and consequently they cycle through a wide RH range (often including saturation if a cloud layer is present) [118].

If the organic mixture does indeed form a single phase at equilibrium, then the conditions for complete equilibration require equal composition in each particle. Actually attaining this equilibrium requires mass exchange, which in turn can occur only through coagulation (which is not really an exchange mechanism) or interparticle mass transfer (condensation–evaporation) [39]. Strict equilibration would require that all species be present in (the organic fraction of) all particles in equal abundances; however, we can also define a "volatility equilibrium" in which particles are neither growing nor shrinking because their "volatility composition" is equilibrated even though their exact composition is not. Specifically, within the VBS the mass fraction of each VBS bin represented in each particle would be the same, so the fraction of semi-volatiles in each particle would be the same. A trivial example of this is a suspension of single-component particles in which some particles have an isotopic label. The particles would be at all times in volatility equilibrium and there would be no driving force for a net mass change, and yet to reach full equilibrium the isotopic composition of each particle would need to become identical, driven by the entropy of mixing.

The concept of volatility equilibration is important when considering very low volatility constituents in particles. The timescale for equilibration of extremely low volatility molecules via net condensation approaches infinity; the molecules will simply never leave their initial particles. However, the more volatile molecules in a mixture can still attain volatility equilibrium by independently establishing equal activity over all particles long before the less volatile constituents have been able to equilibrate. The overall timescale for this process may be complex as different constituents evolve simultaneously.

Condensation, Aging, and Mixing

Mixing for atmospheric aerosol essentially always involves some form of condensational uptake to particles. A unique characteristic of condensational uptake is that it is proportional to the (modified) surface area of particles and not their volume ("modified" refers to the Fuchs correction for gas-phase diffusion for larger particles with $Kn \lesssim 1$, which reduces the effective surface area for condensation). Because the surface area to volume ratio of particles increases as their diameter decreases, condensation tends to have a larger effect on smaller particles, when measured on a mass (or volume) basis. The concept of "surface limited" vs "volume limited" aging has been used before to diagnose different processes in aerosol evolution [119]. However, condensation also tends to drive mixtures out of equilibrium, as the volume fraction of condensing vapors will grow more rapidly for smaller particles than for larger particles. This can be a very useful diagnostic of mixing effects in particles. As an example of "pure condensation" we shall discuss condensation of SOA from the α-pinene + ozone reaction onto pre-existing ammonium sulfate "seed" particles, and then we shall discuss two other cases with more interesting mixing effects.

The condensation rate of organics to a particle surface is given by Eq. 3, multiplied by the saturation ratio of the organic vapors $(S = C_{\mathrm{i}}(\mathrm{gas})/C_{\mathrm{i}}^{*})$ [75]. In Fig. 6 we show the theoretical condensation of organic vapors to inert seeds with an initial lognormal mass mode centered at 300 nm and a Gaussian width of 0.2. The vapors condense onto the inert seeds in proportion to the diffusion-modified seed surface area. The figure shows the initial and final total aerosol size distributions (dashed curves) as well as the final mass distribution of condensed organics and inert seeds (labeled "sulfate" because we tend to use ammonium sulfate for seeds). In the final distribution the condensed organics strongly favor the smaller particles.

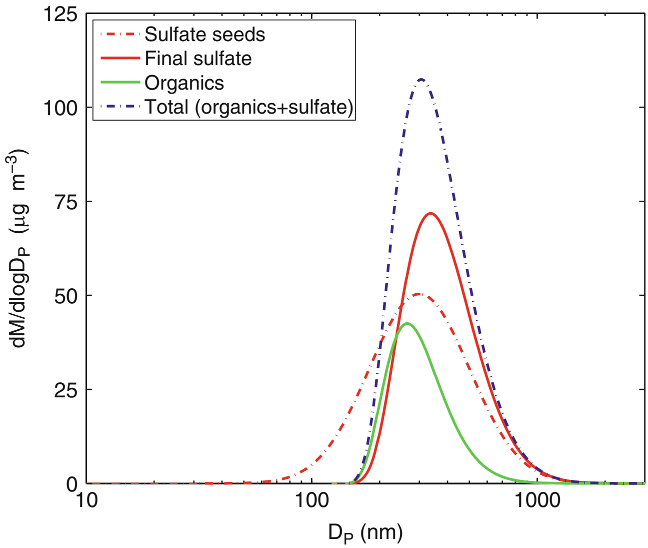

Fig. 6 Calculated condensational growth of organics onto inert (sulfate) seeds, shown as mass distributions vs log of particle diameter. Initial seeds are shown as a *dashed red* Gaussian centered at 300 nm. The final total size distribution is shown as a dashed blue curve. The final sulfate mass distribution is shown as a *solid red curve*, shifted to a 370-nm mode because of organic condensation. The final organic mass distribution is shown as a solid green curve. The organic mass mode after condensation is at 270 nm because condensation (of organics in this case) strongly favors smaller particles with larger surface area to volume and less inhibition from gas-phase diffusion. Because the organics and sulfate do not form a mixture, the final composition (organic:sulfate) is a strong function of particle diameter

This weighting toward smaller sizes of a purely condensational process is characteristic of the interaction between condensing vapors and an inert seed (or of completely non-volatile condensation). It is what drives "condensational narrowing" [120] which is evident in the distorted final distributions in the simulation. In either case the composition of the particles is a strong function of size: in Fig. 6 the 200-nm particles are more than 80% organic, while the 500-nm particles are less than 20% organic; if the particles comprised a single condensed phase they would be far out of equilibrium.

Many SOA formation experiments use inorganic seed particles to encourage condensation onto suspended particles instead of chamber walls [121]. Often the assumption in these experiments is that the inorganic seeds do not influence the SOA mass yields, and mass-yield data confirm this assumption [122]. In Fig. 7 we show size-resolved mass spectra obtained using an aerosol mass spectrometer in particle time of flight (pToF) mode for SOA formed from the toluene + OH reaction and condensed onto dried ammonium sulfate seeds at 15% RH from experiments reported in Hildebrandt et al. [123]. The pToF data show exactly the features expected for condensation onto inert seeds. Very similar data are shown in Prisle et al. [124] for SOA formed from α-pinene + ozone. It is worth noting that

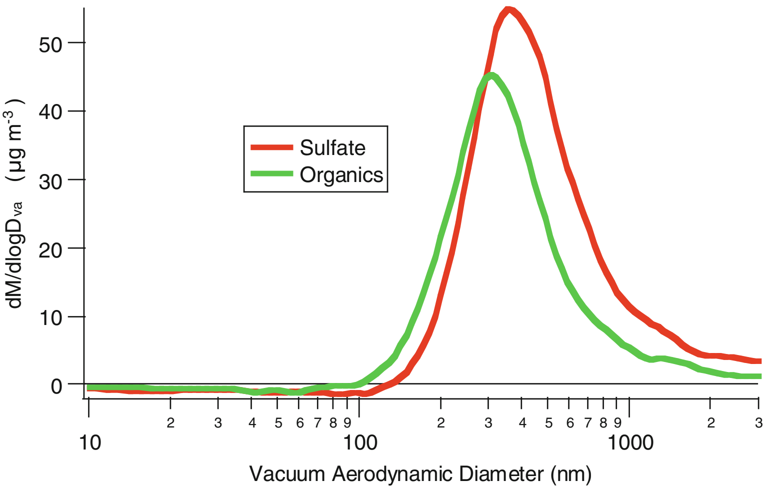

Fig. 7 Measured organic (*green*) and sulfate (*red*) mass distributions from Aerosol Mass Spectrometer particle time of flight (AMS pToF) data. Data are for SOA from toluene oxidation in the presence of ammonium sulfate seeds. Observations closely follow predictions shown in Fig. 6

ambient particles often do *not* show this displacement between organics and sulfate because *both* the organics and sulfate accumulate via condensation, often more or less simultaneously. How particles anneal to a phase-separated morphology with distinct inorganic and organic phases (if indeed this is the equilibrium state [125, 126]) remains unclear.

The situation is very different when organics mix with each other. In Fig. 8 we show AMS pToF data from a mixing experiment first reported by Asa Awuku et al. [60]. In this case POA from a diesel engine was injected into a chamber containing SOA from α-pinene + ozone. As shown in the top panel, the POA initially appeared as a distinct mode with ion fragments characteristic of primary emissions and a modal diameter significantly smaller than the SOA particles. Within 5 min the distinct POA mode vanished and the characteristic ion fragments migrated to the SOA mode, as shown in the lower panel. This clearly indicates that relatively volatile POA evaporated and re-condensed into the SOA, with the lower activity of the POA species in the SOA particles acting as a thermodynamic driving force for the mixing. There were, however, strong indications that the mixing was non-ideal. Both composition and concentration influenced these effects. Specifically, an injection of motor-oil droplets similar to the diesel POA remained stable for hours as a distinct mode while the diesel POA quickly mixed with the SOA seeds. The activity coefficients of the oil vapors were thus significantly greater than 1 in the SOA particles, so at some finite concentration of POA species in the SOA (and vice versa, though the mass spectra did not show this directly) the suspension became stable, with two distinct condensed phases present [60]. Also, the rapid (5 min) mixing of a significant quantity of POA into the SOA particles clearly shows that (in this case at least) diffusion of the POA species into the SOA was not a

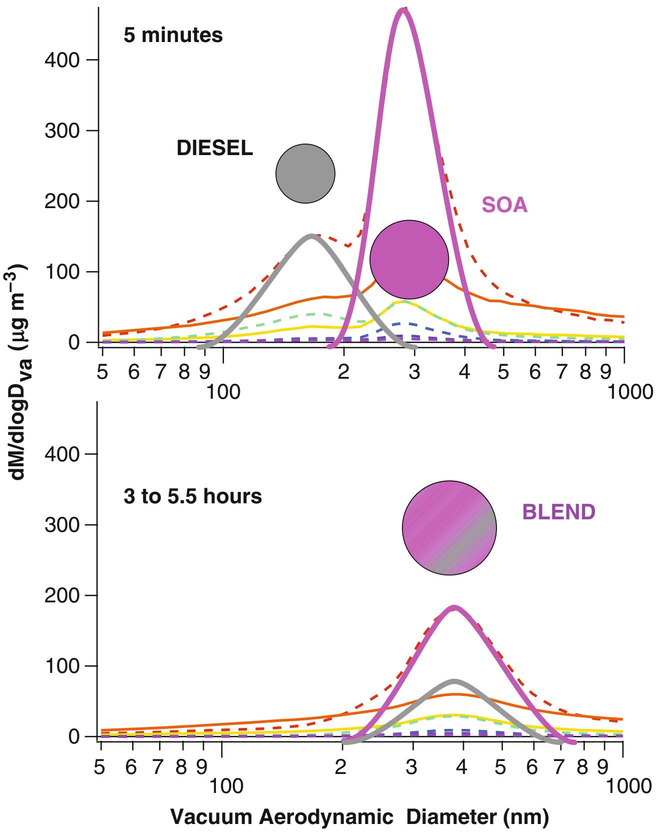

Fig. 8 Measured AMS pToF distributions for diesel POA particles injected into a smog chamber containing SOA from α-pinene ozonolysis. POA particles are evident as a distinct mode at 180 nm for only 5 min (*upper panel*) after which they vanish into the SOA seeds (initially at 300 nm, ultimately at 400 nm, *lower panel*). Both the timing and coincident size distributions of the ultimate particle distribution confirm that mixing of POA into SOA occurred via evaporation of fresh POA and subsequent condensation and full (volume) mixing into the SOA seeds

significant impediment; the lack of complete mixing in some cases likely indicates non-ideality as opposed to delayed equilibration.

A final example involves gas-phase aging chemistry. In Fig. 9 we show two pToF spectra from semi-volatile diesel oxidation experiments described elsewhere [127–129]. In these experiments, diesel emissions were diluted to near ambient levels and then exposed to photolytically generated OH radicals [128]. The pToF data are shown for two key ion fragments, $m/z = 57$ and 44, which are traditionally indicative of reduced ("hydrocarbon like") POA and oxidized SOA [130]. In these experiments the total OA concentrations more than doubled in 5 h due to SOA formation. The figure reveals that the $m/z = 44$ marker characteristic of the SOA remained locked into the mode characteristic of the POA defined by $m/z = 57$, even as the $m/z = 44$ abundance increased due to condensation. Data are shown just

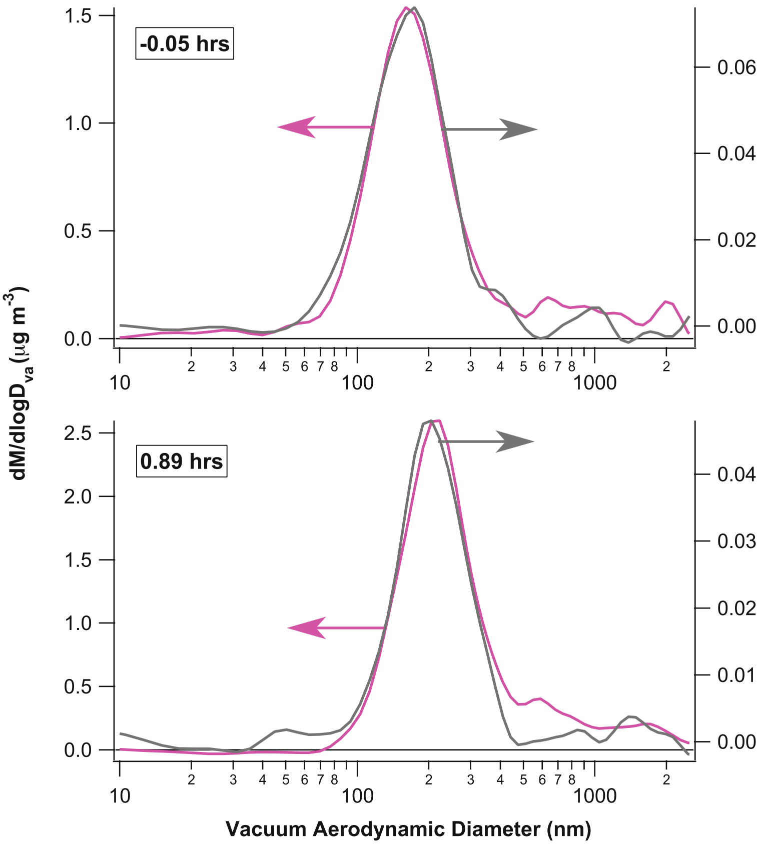

Fig. 9 SOA production on diesel seed particles. SOA formed from photooxidation of diesel vapors shown by increasing mass fraction of $m/z = 44$ (largely CO_2^+, *pink*) fragment, left scale vs $m/z = 57$ (largely $C_4H_9^+$, *gray*) fragment, right scale. The *horizontal arrows* point toward each axis at a constant *y* value in the two panels to illustrate the extent of condensation by SOA. Concurrent diameter growth shows that condensation and evaporation maintain equal mass fractions of more reduced and more oxidized organic species in all particles, independent of size

before oxidation and after 1 h of photochemistry, but the OOA mode never lagged behind the POA mode in the manner characteristic of condensation to inert seeds shown in Figs. 6 and 7. The evidence is thus strong that the POA and SOA formed a mixture throughout the diesel oxidation experiment.

To maintain the equal mixing shown in Fig. 9, condensation alone is not sufficient; the only way to keep the volume (mass) distributions of species constant during a period of strong condensational growth is via *net* condensation, meaning that some species also evaporate significantly from relatively enriched particles and re-condense on relatively depleted ones. From these data there is no way to tell whether it was the POA or the SOA species (or both) evaporating and recondensing, only that this surely occurred with more or less complete volume mixing on a timescale faster than the growth (faster than 1 h or so). However, if the mixing experiment shown in Fig. 6 and the calculations shown in Fig. 3 offer any indication, it is likely that the POA vapors were largely responsible for this equilibration.

4 Aging

The previous example brings us to aging. Here "aging" refers to chemical aging – in other words chemical reactions that alter the composition of an organic aerosol. There are at least five modes of aging: gas-phase oxidation of organic vapors, heterogeneous uptake of oxidants, condensed-phase reactions among organics, acid–base reactions involving organics, and aqueous reactions involving organics. As discussed in the introduction, the focus of this work is largely on gas-phase aging.

4.1 Gas-Phase Oxidation

Gas-phase chemistry is a key player in organic-aerosol evolution. We shall discuss organic oxidation chemistry first because this is a homogenous process. There are no circumstances where it will not happen – no diffusion limitations or other inhibiting phenomena. If an organic compound is oxidized in the gas phase and an oxidation product has a sufficiently low C^*, that product will condense to a particle when it collides with it. Thus, when we consider gas-phase oxidation we are interested principally in the volatility distribution of the reaction products as well as their composition. All increases in OA mass due to gas-phase chemistry can be called "secondary organic aerosol" (SOA) because the reaction products are secondary molecules and the aerosol mass increases, so the added mass is secondary mass. These topics have been extensively covered in numerous publications and reviews, and so we shall touch only briefly on key issues here. For historical and practical reasons we shall split our discussion between SOA formed from volatile precursors (sometimes called "traditional" SOA) and SOA formed from less volatile precursors (one class of so-called "non-traditional" SOA). Hydrocarbon oxidation is an inexorable process proceeding from a highly reduced primary compound (often relatively volatile) ultimately to CO_2 (also highly volatile) [65]; however, intermediates in this process can have extremely low vapor pressures.

4.1.1 VOC Secondary Organic Aerosol

SOA from VOCs has a long history [15, 17, 51] and is also discussed elsewhere in this volume. The key finding relevant to a broader aging discussion is that products of gas-phase oxidation reactions can have lower C^* than the precursor. A recent focus has been to conserve carbon when parameterizing an SOA formation process, i.e., in a VBS formulation

$$\mathrm{VOC} + \mathrm{Ox} \rightarrow \left\{\alpha_i\, C_i^*\right\},$$

where $\{\alpha_i\}$ is a set of carbon mass yields (i.e., micrograms per cubic meter of OC formed for 1 μg m^{-3} of VOC consumed). The total OA mass can then be obtained with some added information – specifically $OM{:}OC_i$, the ratio of organic mass to organic carbon within each product bin. This can be estimated from loading-dependent composition (C:H:O) measurements during SOA formation [131] and is directly constrained within a 2D formulation of the VBS that includes composition information as a second dimension [63, 64].

The relevant issue here is that many analyses suggest that much of the SOA mass is semi volatile, as discussed above. In addition, because the SOA mass yields are generally well below 1, it is clear than many other reaction products are lower in volatility than the precursor but too volatile to influence the SOA mass. All of those vapors are in play for subsequent later-generation aging chemistry.

4.1.2 IVOC and SVOC Secondary Organic Aerosol

Intermediate volatility organics (IVOCs) are much less volatile than VOCs but still much more volatile than species that can condense under ambient conditions. Most of the first-generation SOA products shown in the VBS fits in Fig. 10, with $300 < C^* < 3 \times 10^6$ μg m^{-3}, are considered IVOCs. In addition, a substantial fraction of primary emissions from high-temperature combustion, including wood burning, food preparation, internal combustion engines, and turbine engines, consists of IVOCs and SVOC (with $0.3 < C^* < 300$ μg m^{-3}) [90]. We shall discuss direct formation of SOA from IVOC and primary emissions first because the kinetics and initial mechanisms of these reactions have been studied more widely.

SOA from Primary IVOC Emissions

A challenge with the atmospheric chemistry of IVOC is the exponential increase in chemical complexity with increasing carbon number, even for "simple" hydrocarbons containing only carbon and hydrogen [35]. Consequently, studies of SOA formation from IVOCs fall into two categories: study of individual molecules or sequences of molecules as representative model systems and study of undifferentiated "whole" emissions diluted to near ambient conditions to encourage atmospherically relevant partitioning of the primary emissions.

Two broad classes of lower volatility hydrocarbons have been studied extensively: alkanes and polycyclic aromatics. Alkanes have been more systematically treated with regard to their potential for SOA formation, while the chemistry and phase partitioning of polycyclic aromatics were in many ways the foundation for the ambient partitioning theory described in this chapter because of the significant concerns over PAH health effects.

Alkanes

Alkanes are an excellent model system because they present a homologous sequence in both carbon number (and thus volatility) as well as structure (and thus varying chemical behavior). Alkane SOA formation has been studied systematically by Ziemann and coworkers [132] as well as others. Broadly, the SOA formation potential of *n*-alkanes increases systematically with carbon number [132, 133] as the precursor volatility decreases. Substitution in the form of branching significantly decreases SOA formation at a given carbon number, while cyclization increases SOA formation. In each case the reason is fragmentation of secondary products: branched alkanes are more vulnerable to C–C bond cleavage during oxidation, while cycloalkanes can sustain one C–C bond cleavage event without a decrease in carbon number because of the tethering effect of the cyclic structure [134].

Polycyclic Aromatics

PAHs have been studied for decades because of their high potential for negative health effects [135–137]. Investigators quickly realized that PAH volatility spanned a wide range and thus that important PAH species would be found in both the gas and condensed phases in the atmosphere. Partitioning theory was developed for atmospheric applications in large measure to address these issues. For some time, adsorption to surfaces was considered to be more important than absorption into an organic condensed phase [138]; however, by stages it became evident that the total mass of the condensed phase (TSP) was significant to partitioning [139] and ultimately that absorptive partitioning with the condensed organic phase was often the appropriate framework for partitioning [140]. While that work laid the foundation for the perspective on partitioning described here, consideration of the SOA formation from PAH oxidation is much more recent. Like the alkanes, PAH oxidation has been studied as a potentially important model for SOA formation from IVOCs [141].

Evaporated Primary Emissions

Real primary emissions consist of a complex mixture including linear and branched alkanes, mono aromatics, substituted aromatics (alkyl benzenes), and PAHs, among many other compounds [7, 142]. The most direct evidence that SOA formation is important for typical atmospheric IVOC mixtures thus comes from experiments on vapors from these very mixtures [127, 143–148].

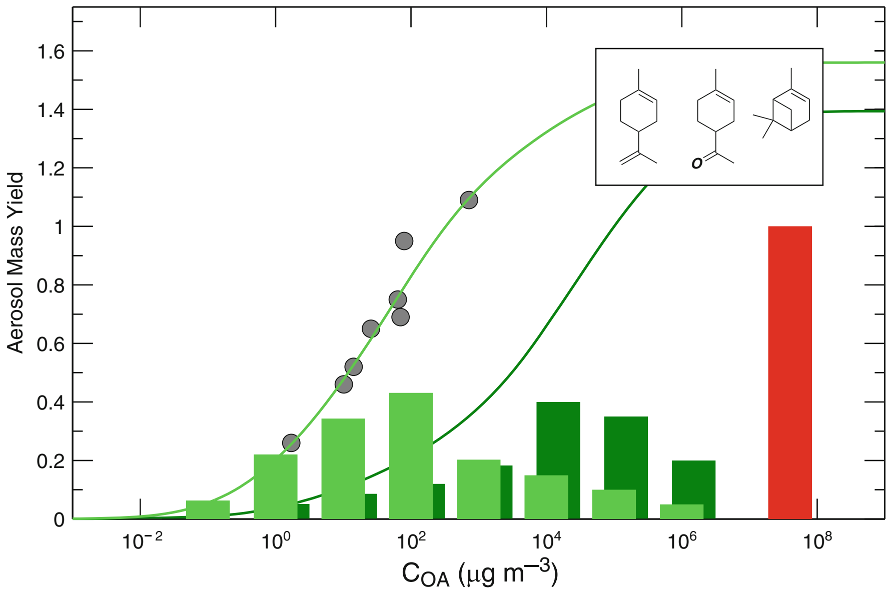

Fig. 10 SOA product volatility distributions for α-pinene and limonaketone in *dark green* and mass yields vs C_{OA} as *dark green curve*. Precursors with similar volatility, structure, and chemistry have similar yields. Product volatility distribution and yields for D-limonene ozonolysis are shown as *light green bars* and a *light green curve* (and *gray* data points). Oxidation of the additional exocyclic double bond in limonene results in substantially less volatile SOA products and correspondingly higher SOA yields

4.1.3 Aging of VOC SOA

All of the first-generation vapors from VOC SOA will certainly undergo further gas-phase oxidation, which will in turn influence the phase partitioning thermodynamics of the OA mixture, i.e., gas-phase aging of SOA.

Multiple Ozonolysis Generations

Several forms of aging of SOA vapors have been observed. One clear form is oxidation of multiply unsaturated alkenes. Many terpenes have multiple unsaturations, and in some cases different double bonds have very different rate constants for reaction with ozone. Examples include terpinolene, myrcene, limonene, α-humulene, and β-caryophyllene [149, 150]. In these systems, ozone will react with one double bond in the terpene and produce some SOA. However, after the precursor is completely removed, SOA levels can continue to rise as the first-generation semi-volatile products continue to react with ozone to produce less volatile second-generation products [149].

Limonene is a revealing example. It is similar to α-pinene in possessing a methyl-substituted endocyclic double bond in a six-member ring, but in addition it has an exocyclic terminal unsaturation. Figure 10 shows SOA mass-yield data and a corresponding VBS product distribution (in light green) for the limonene + ozone reaction under low-NO_x conditions [150]. The inset shows structures for limonene, limona ketone, and α-pinene. The darker green histogram and yield curve is valid for α-pinene and limona ketone, which generate almost identical SOA mass distributions after ozonolysis [38]. Initial ozonation of limonene also produces SOA much like α-pinene and limona ketone, but subsequent ozonation of the exocyclic double bond in the first-generation products strongly favors the ketone-oxide over the ketone moiety shown in limona ketone and consequently forms substantially less volatile second-generation products [150–152]. As Fig. 10 shows, the resulting product distribution is two to three orders of magnitude less volatile than typical first-generation terpene ozonolysis products, which is consistent with additional peroxide and carboxylic acid functionality [153] greatly offsetting the loss of one carbon from the terminal methylene.

An interesting wrinkle in the limonene story is that the second ozonolysis reaction can be heterogeneous. The fresh SOA produced when ozone reacts with the endocyclic double bond is unsaturated [153], but under low-NO_x conditions it reacts much more rapidly than is plausible based on gas-phase kinetics, but at a rate consistent with a heterogeneous ozone uptake coefficient of roughly 10^{-3} [150]. Under high-NO_x conditions the SOA (which contains organic nitrate functionality) has a much lower heterogeneous reactivity to ozone and consequently species remain in the gas phase that oxidize at a rate consistent with the ozonolysis of terminal double bonds, forming second-generation SOA more slowly, long after the limonene itself has been completely oxidized [150].

Multi-generation OH Oxidation

Oxidation by OH radicals (or photooxidation in general) is much more difficult to deconvolve than ozonolysis because there is seldom the clear separation in timescales that can appear in the ozonolysis aging just discussed. However, later-generation oxidation by OH is likely to be much more important in the atmosphere because it is ubiquitous. OH will react with essentially all organic molecules, though the kinetics and mechanisms of the highly substituted species typical of first-generation and later-generation oxidation products remain highly uncertain. Nonetheless, there is no doubt that these reactions will occur, and little doubt that they will be quite rapid, in most cases oxidizing semi-volatile vapors within hours [64].

Multiple-generation oxidation has been studied theoretically via mechanism generators that apply structure activity relations for rate constants and product distributions [49]. Several specific tracers of later-generation oxidation have been proposed. One is a C_8 triacid formed via gas-phase oxidation of *cis*-pinonic acid, which is itself a first-generation oxidation product of α-pinene [154]. The triacid is produced rapidly when gas-phase *cis*-pinonic acid is exposed to OH radicals, but not when the pinonic acid is partitioned into SOA at low temperatures [155]. For bulk SOA characteristics, Chhabra et al. [156] have shown that SOA formation from oxidized precursors results in SOA whose mass spectrum is higher in the f_{44}–f_{43} "triangle" space recently proposed as a diagnostic for ambient OA processing [157].

In the recent multiple chamber chemical aerosol aging study (MUCHACHAS), first-generation SOA was produced from α-pinene + ozone and then exposed to OH radicals in a subsequent, separate step [112, 113, 155, 158–160]. The OH exposure caused a substantial jump in SOA mass concentrations [112, 113, 158] and significant changes in SOA volatility and hygroscopicity [112, 113, 159]. This controlled experiment strongly confirmed that long-term gas-phase aging by OH radicals can substantially alter OA properties.

There is thus compelling evidence that gas-phase OH oxidation will age OA by oxidizing semi-volatile vapors as well as slightly more volatile IVOC intermediate products. This will occur throughout the atmosphere with a rate constant estimated to be of order 2×10^{-11} cm^3 molec^{-1} s^{-1}, giving a lifetime for typical OH concentrations of order 8 h [92, 158]. Other aging mechanisms can be scaled by this ubiquitous value to assess their relative importance.

4.2 *Heterogeneous Aging*

A large body of work addresses aging of organic particulate matter via heterogeneous uptake of oxidants, especially OH and ozone. Just as partitioning theory progressed from a focus on adsorptive to absorptive behavior, heterogeneous uptake has been viewed in terms of uptake of oxidants controlled by Langmuir-Hinshelwood type adsorptive isotherms [79, 161], but diffusion of oxidants into a bulk aerosol has also been considered in various contexts [162]. Heterogeneous formulations can differ depending on whether the principal focus is the loss of an oxidant upon uptake [87] or the loss of condensed-phase constituents due to oxidant uptake [163–166]. The "Pöschl Rudich Ammann" framework was initially presented with a principal focus on gas–surface interactions for multiphase processes, but has recently been extended to resolve diffusion into a spherically symmetric bulk as well [87]. The objective here is not to review even a small portion of the literature on heterogeneous oxidant uptake but to focus on the interplay between heterogeneous oxidation and organic phase partitioning.

Heterogeneous oxidation by OH is intrinsically slower than homogeneous gas-phase oxidation of organic vapors, since most molecules in a given particle are shielded from gas-phase radicals colliding with the surface. A rate constant for the gas-phase reaction of OH radicals with large organic species of 2×10^{-11} cm^3 molec^{-1} s^{-1} is at least ten times larger than that of gas-phase OH with an organic species within a submicron particle [92]. The rate at which a molecule will undergo oxidation in each phase is a function not only of these rate constants but also by its abundance (as measured by mole fraction) in each phase. This is illustrated in Fig. 11 which shows the effective oxidation rate constant in each phase as a function of volatility as well as the total rate constant including

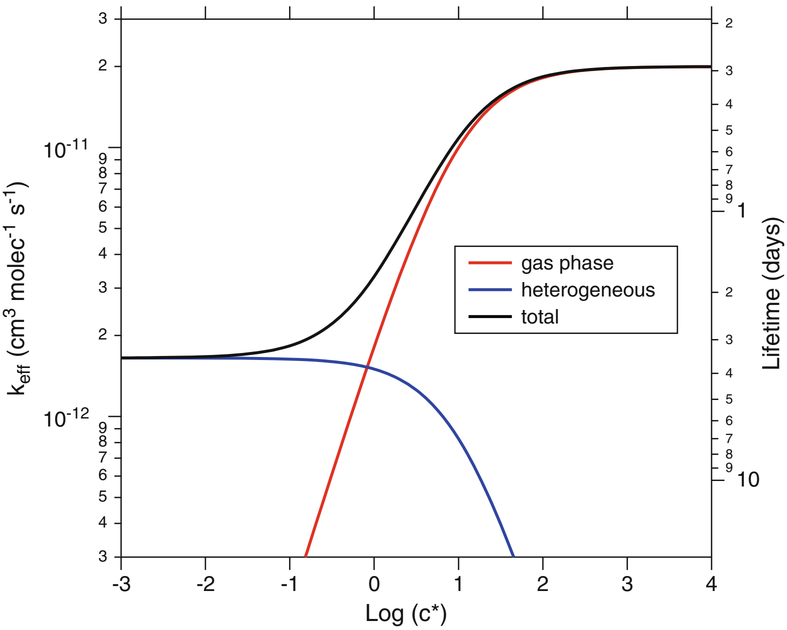

Fig. 11 Effective OH oxidation rate constants for organics in gas phase (*red curve*) and condensed phase (*blue curve*) for a gas-phase OH rate constant of 2×10^{-11} cm^3 molec^{-1} s^{-1} and a heterogeneous OH uptake coefficient of 1, for 200 nm diameter particles and 10 μg m^{-3} total organic aerosol. Results are given as equivalent gas-phase values, modified by the fraction of organics in each phase and diffusion limitations of gas-phase OH to condensed-phase organics. Oxidation lifetimes (in days) are given on left-hand *y* axis, for 2×10^6 OH cm^{-3}

oxidation in either phase. Rates were calculated assuming a gas-phase rate constant of 2×10^{-11} cm^3 molec^{-1} s^{-1}, reactive uptake coefficient (γ) of 1, particle diameter of 200 nm, and organic aerosol loading (C_{OA}) of 10 μg m^{-3}. The figure shows that gas-phase oxidation will almost always dominate over heterogeneous oxidation unless the molecule is very low in volatility (C^* of 0.1 μg m^{-3} or lower). Molecules almost wholly in the condensed phase of course can only be oxidized there. It is important to note that the heterogeneous timescale of 3–4 days is still shorter than the characteristic atmospheric residence time of submicron particles of 1 week or more [167]. Consequently, heterogeneous oxidation is still clearly an important process for organic compounds contained within aerosol particles.

In addition to providing insight into the kinetics of multiphase aging, studies of heterogeneous oxidation also serve as indirect probes of the mixing effects discussed earlier. Measuring the rate and extent of degradation of individual aerosol components provides information not only on molecular-level reactivity but also on mixing within the particle. This is because the reactive-diffusive length of OH in organic particles is of order 1 nm [168], and so heterogeneous OH reactions will be confined to the particle surface. For example, in a study of the multigenerational heterogeneous oxidation of squalane ($C_{30}H_{62}$), squalane degradation followed a simple pseudo-first-order kinetics (exponential decay) over multiple oxidation lifetimes, with concentrations eventually falling to zero [169]. Similarly, the first and second generation products reacted away at the same rates. This indicates that, at any given time, a sufficient amount of reactant (squalane and early-generation products) is present at or near the surface of a (pump oil) particle to react with OH; mixing within the particle is thus very fast on the timescale of the experiment (37 s). A similar conclusion can be drawn for heterogeneous oxidation of α-pinene SOA by OH. Experiments with very high SOA concentrations (which favors the condensed phase and thus heterogeneous oxidation) and very high OH exposure in 37 s found almost complete conversion of fresh SOA into highly aged material. The aged aerosol strongly resembled ambient low-volatility oxidized organic aerosol (LV-OOA) while maintaining almost no correlation with the original fresh SOA mass spectrum [30]. This would not be possible unless essentially all of the organic species within the particles were able to diffuse to the particle surface (or even evaporate) in 30 s or less. On the other hand, in similar experiments on the heterogeneous oxidation of levoglucosan ($C_6H_{10}O_5$) and erythritol ($C_4H_{10}O_4$), the reactants were not totally lost after an initial rapid decay, consistent with the formation of viscous materials with mixing timescales of at least several minutes. This serves as an illustration that generalizations about diffusion limitations within organic particles may be very difficult to draw, as the specific particle composition (including organics, inorganics, and water) as well as temperature may alter constituent diffusivities by many orders of magnitude.

Heterogeneous oxidation experiments also allow for the investigation of the possibility that organic condensation may "coat" existing particles, isolating the core of the particle from the surrounding gas. Such a coating implies a lack of mixing between the condensing vapor (the coating material) and the particle core, but this can be a dangerous assumption if the two are miscible. One example of this is shown in Fig. 12, which is a relative kinetics plot of particle-phase cholestane loss compared to gas-phase oxidation of meta-xylene by OH radicals [143]. For the reasons discussed above, it is reasonable to regard heterogeneous loss of condensed-phase organics as a fairly precise surface probe. Figure 12 shows two things. First, coating of POA particles containing cholestane by a nominally quite thick layer of α-pinene SOA did nothing to slow down heterogeneous cholestane loss, suggesting that the SOA formed a uniform mixture with the POA. That is consistent with the mixing experiments described above [60]. Second, cholestane loss slowed significantly at high RH (~75%), suggesting that an aqueous surface layer formed, excluding nonpolar compounds such as cholestane. This is consistent with recent findings that two distinct condensed phases form for wet OA particles as long as the O:C of the organics is below approximately 0.7 [125, 126].

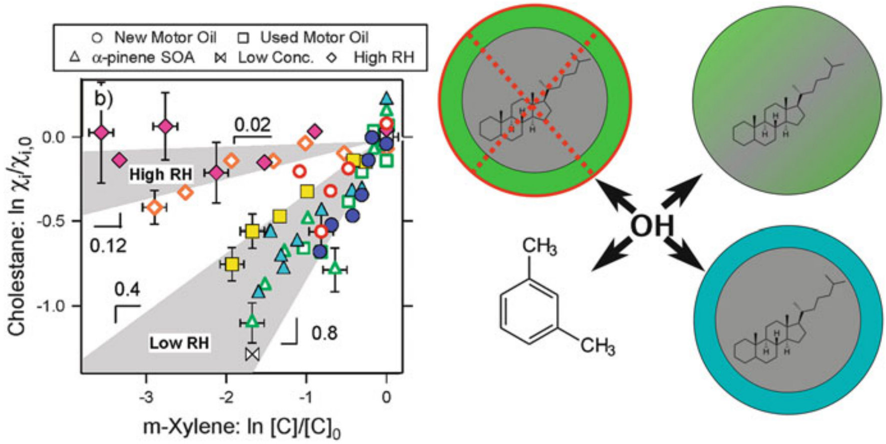

Fig. 12 Relative oxidation rates by OH radicals of condensed-phase cholestane vs gas-phase *m*-xylene in different organic-aerosol matrices, all of which include a high fraction of motor oil. Cholestane oxidation is independent of OA concentration or the presence of a substantial SOA "coating" consisting of up to half of the total particle mass. However, high relative humidity slows cholestane oxidation by an order of magnitude. This suggests that a thin film of water on oil can significantly retard cholestane oxidation, perhaps by excluding the cholestane from the particle surface; the SOA, on the other hand, does not coat the particle surface but rather mixes with the oil and thus does not impede cholestane oxidation

4.3 Aqueous-Phase Aging

In recent years there has been intense interest in the formation and evolution of atmospheric particulate matter within the aqueous phase [170]. Such processes occur by dissolution of organics into a water droplet (deliquesced particle or cloud droplet) followed by oxidation by a dissolved oxidant (most likely OH). Studies of these pathways have been reviewed in detail very recently [118, 171] and so will not be discussed here; instead, as in the previous section, the focus here is on the relationship between partitioning and aging chemistry.

The relative importance of the gas and the aqueous phases as media for the oxidation of organic species depends critically on the fraction of the species present in each phase. This in turn is a function both of the compound's intrinsic tendency to partition between each (as described by its effective Henry's Law Constant, H^*) and the concentration of liquid water present [118]. Thus partitioning into the aqueous phase is governed by the same general considerations as partitioning into the organic phase (which is governed by saturation vapor pressure and organic aerosol loading). In fact, the Henry's Law solubility of a compound is really just a measure of the volatility of that compound over water. As with purely organic mixtures, Raoult's law will apply for ideal solutions, but the activity can be strongly modified by some activity coefficient related to the interaction of that species with water. Accordingly, it is useful to express the Henry's Law solubility as volatility

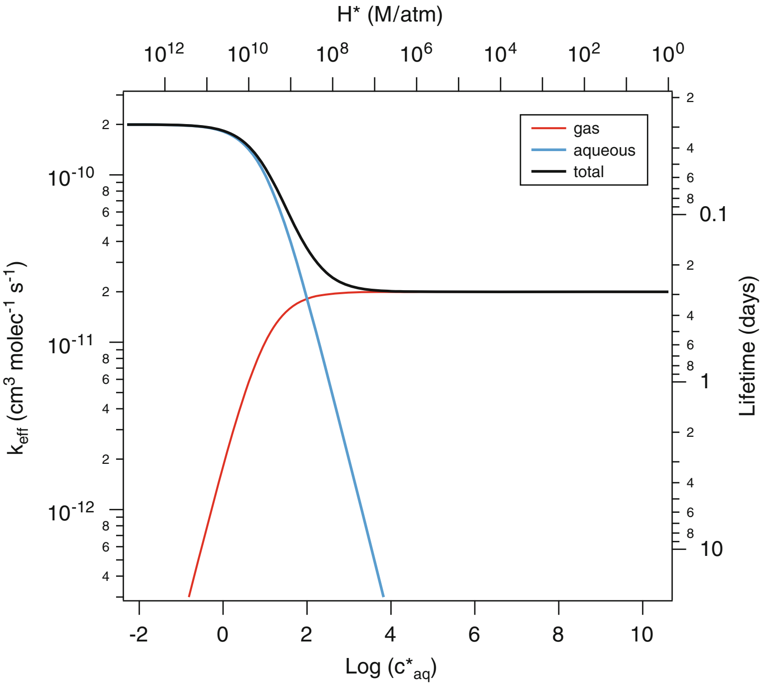

Fig. 13 Effective OH oxidation rate constants for organics in gas phase (*red curve*) and aqueous phase (*cyan curve*) for a gas-phase rate constant of 2×10^{-11} cm^3 molec^{-1} s^{-1} and an effective aqueous-phase OH rate constant of 2×10^{-10} cm^3 molec^{-1} s^{-1}. The principal abscissa is the effective saturation concentration with respect to dissolution in 10 μg m^{-3} of liquid water. Oxidation lifetimes (in days) are given on the left-hand *y* axis, for 2×10^6 OH cm^{-3} in the gas phase

(micrograms per cubic meter), for comparison with the liquid water content (just as C^* can be compared to C_{OA}). Following Ervens et al. [172], this volatility over water is called C^*_{aq}, and is equal to $(R\,T\,H^*/\rho_w)^{-1}$, where H^* is the effective Henry's Law constant (M atm^{-1}), T is temperature (K), R is the gas constant (0.08206 L atm K^{-1} mol^{-1}), and ρ_w is the density of water (10^{12} μg m^{-3}).

Figure 13 shows the effective rate constants for gas-phase and aqueous-phase oxidation as a function of C^*_{aq} (and H^*), assuming a liquid water content (C_w) of 10 μg m^{-3} (a typical ambient value for deliquesced aerosol). This is directly analogous to Fig. 11, which shows the rates of heterogeneous vs gas-phase oxidation as a function of C^*. As in Fig. 11, the gas-phase OH rate constant is set at 2×10^{-11} cm^3 molec^{-1} s^{-1}. The effective aqueous-phase OH rate constant is chosen to be ten times higher at 2×10^{-10} cm^3 molec^{-1} s^{-1}), reflecting the possibility that aqueous OH concentrations may be higher than in the gas phase [173]. (The actual aqueous-phase rate constants can be quite variable, but are generally similar to those in the gas phase [173].) Even with this higher rate, aqueous-phase oxidation will dominate only when the molecule of interest is exceedingly water soluble ($H^* > 7 \times 10^8$ M atm^{-1}) due to the small amount of liquid water available. Most atmospheric species, even those that are considered to be highly water-soluble (such as glyoxal, glycolaldehyde, and diacids), have H^* well below this threshold [174], and thus will not partition sufficiently into the aerosol aqueous phase to undergo significant aqueous-phase aging under these conditions.

There are several important caveats to this analysis, however. First, OH concentrations in the aqueous phase are highly uncertain, since there are no measurements of [OH] in deliquesced particles or cloud droplets. If aqueous OH concentrations are still higher than indicated in Fig. 13 (as suggested by some models [173]), the threshold for aqueous-phase oxidation would move to higher values of C^*_{aq} (lower values of H^*); on the other hand, if aqueous OH concentrations are lower (as suggested by other models [170]), even lower values of C^*_{aq} (higher values of H^*) would be needed for aqueous oxidation to dominate. This highlights the need for an improved understanding of oxidant concentrations in the atmospheric aqueous phase. Unless there is substantial radical recycling (OH regeneration) in the aqueous phase, aqueous oxidation by OH will be subject to the same diffusion limitations on heterogeneous oxidation.

A second caveat involves the effect of liquid water content C_w; the value used (10 μg m^{-3}) is reasonable for ambient fine particulate matter but would be orders of magnitude higher for cloud water (with C_w as high as 1 g m^{-3}). Under such conditions, partitioning into the aqueous phase will happen for much more volatile species (H^* of 7×10^4 M atm^{-1} or higher), including the water-soluble species mentioned above. Third, this analysis assumes that Henry's Law accurately describes partitioning between the gas and aqueous phase, independent of aqueous-phase concentrations. In reality, the high concentrations in the aerosol aqueous phase are likely to introduce substantial deviations from ideality; these substantial activity coefficients could have a dramatic (and uncertain) effect on partitioning. Finally, under some conditions, particles may include multiple phases [125, 175], so that partitioning between at least three phases (gas, organic, aqueous) must be considered. In such cases the simple two-phase picture in Fig. 13 (or Fig. 11) is insufficient to describe the aging chemistry of the entire system, as the relative values of C^*, C^*_{aq}, C_{OA}, and C_W must be considered when predicting the equilibrium phase of the organic species.

In spite of all these uncertainties, the description of aqueous oxidation in terms of simple partitioning (Fig. 13) clearly shows that only molecules with very large Henry's Law solubilities can undergo significant oxidation in the aqueous phase. This includes highly water-soluble species such as glyoxal, at least when aqueous [OH] and/or liquid water content is high, but categorically excludes all hydrocarbons as well as most monofunctional organic species that have more than one carbon [174]. It also points to the need to run laboratory studies of aqueous oxidative processing under atmospherically relevant partitioning conditions, with liquid water contents in the range of 10 μg m^{-3} (for deliquesced particles) to 1 g m^{-3} (for cloud water). To date, most (though not all [176, 177]) laboratory studies of aqueous oxidation have been carried out in bulk aqueous solution, with liquid water contents that are far higher than this, on the order of 10^6 g m^{-3} (the density of liquid water). These studies are unlikely to be representative of the gas-droplet partitioning conditions typical of the atmosphere, and thus may not accurately reflect atmospheric aging.

As with heterogeneous oxidation, aqueous-phase oxidation may play an important role in aging water-soluble organics already present in particles, and it can also play a unique role for a small but important set of highly water soluble, low carbon-number organic vapors [172].

5 Conclusions

Phase partitioning and aging chemistry are inexorably linked when considering the chemical evolution of organic aerosol, both because the phase defines the aerosol and because absolute rate of aging depends strongly on the phase holding an organic compound. A key observation in ambient organic aerosol is that the aerosol becomes highly oxidized very rapidly [30, 178, 179]. Heterogeneous oxidation mechanisms appear to be incapable of oxidizing OA with sufficient speed, while gas-phase oxidation can do so. However, heterogeneous processes still compete favorably with the residence time of OA in the atmosphere and thus certainly play an important atmospheric role. In addition, processes that might simply retard mass transfer between the particle and gas phases appear unable to provide sufficiently rapid oxidation.

Overall, the coupling among these multiphase processes, including chemistry in all phases and the equilibria and dynamics of mass transfer among the phases, needs to be described in detail before we can resolve with certainty the relative role of each process under atmospheric conditions. The timescales for all three processes discussed here – gas-phase, heterogeneous, and aqueous-phase oxidation – are competitive with the residence time of particles in the atmosphere. Gas-phase oxidation will win out for most organic vapors because it is homogeneous and fast, but condensed-phase processes may have a vital role in the full maturation of organic aerosol over longer timescales during long-range transport.

Acknowledgments NMD and ALR are supported by grants from the U.S. National Science Foundation (NSF CHE 1012293 and AGS 1136479) and the Department of Energy (DE-SC0007075). JHK is supported by a grant from the National Science Foundation (AGS 1056225). IR is supported by a grant from the European Research Council (278277) and Vetenskapsrådet. ERT is supported by an NSF doctoral fellowship.

References

1. Hildemann LM, Mazurek MA, Cass GR, Simoneit BRT (1991) Quantitative characterization of urban sources of organic aerosol by high-resolution gas-chromatography. Environ Sci Technol 25(7):1311–1325
2. Schauer JJ, Cass GR (2000) Source apportionment of wintertime gas-phase and particle-phase air pollutants using organic compounds as tracers. Environ Sci Technol 34 (9):1821–1832
3. Mazurek MA, Cass GR, Simoneit BRT (1991) Biological input to visibility-reducing aerosol-particles in the remote arid southwestern United States. Environ Sci Technol 25(4):684–694
4. Rogge WF, Hildemann LM, Mazurek MA, Cass GR, Simoneit BRT (1998) Sources of fine organic aerosol. 9. Pine, oak and synthetic log combustion in residential fireplaces. Environ Sci Technol 32(1):13–22
5. Robinson AL, Subramanian R, Donahue NM, Bernardo-Bricker A, Rogge WF (2006) Source apportionment of molecular markers and organic aerosol. 2. Biomass smoke. Environ Sci Technol 40:7811–7819
6. Rogge WF, Hildemann LM, Mazurek MA, Cass GR, Simoneit BRT (1993) Sources of fine organic aerosol. 2. Noncatalyst and catalyst-equipped automobiles and heavy-duty diesel trucks. Environ Sci Technol 27(4):636–651
7. Schauer JJ, Rogge WF, Hildemann LM, Mazurek MA, Cass GR, Simoneit BRT (1996) Source apportionment of airborne particulate matter using organic compounds as tracers. Atmos Environ 30(22):3837–3855
8. Subramanian R, Donahue NM, Bernardo-Bricker A, Rogge WF, Robinson AL (2006) Contribution of motor vehicle emissions to organic carbon and fine particle mass in Pittsburgh. Pennsylvania: effects of varying source profiles and seasonal trends in ambient marker concentrations. Atmos Environ 40:8002–8019
9. Schauer JJ, Kleeman MJ, Cass GR, Simoneit BRT (1999) Measurement of emissions from air pollution sources. 2. C-1 through C-30 organic compounds from medium duty diesel trucks. Environ Sci Technol 33(10):1578–1587
10. Rogge WF, Hildemann LM, Mazurek MA, Cass GR, Simonelt BRT (1991) Sources of fine organic aerosol. 1. Charbroilers and meat cooking operations. Environ Sci Technol 25 (6):1112–1125
11. Nolte CG, Schauer JJ, Cass GR, Simoneit BRT (1999) Highly polar organic compounds present in meat smoke. Environ Sci Technol 33(19):3313–3316
12. Schauer JJ, Fraser MP, Cass GR, Simoneit BRT (2002) Source reconciliation of atmospheric gas-phase and particle-phase pollutants during a severe photochemical smog episode. Environ Sci Technol 36(17):3806–3814
13. Robinson AL, Subramanian R, Donahue NM, Bernardo-Bricker A, Rogge WF (2006) Source apportionment of molecular markers and organic aerosol. 3. Food cooking emissions. Environ Sci Technol 40:7820–7827
14. Rogge WF, Hildemann LM, Mazurek MA, Cass GR (1994) Sources of fine organic aerosol. 6. Cigarette-smoke in the urban atmosphere. Environ Sci Technol 28(7):1375–1388
15. Paulson SE, Pandis SN, Baltensperger U, Seinfeld JH, Flagan RC, Palen EJ, Allen DT, Schaffner C, Giger W, Portmann A (1990) Characterization of photochemical aerosols from biogenic hydrocarbons. J Aerosol Sci 21:S245–S248
16. Kamens R, Jang MS, Hu JX, Coe D, Strommen M (1996) Equilibrium and atmospheric semi-volatiles. Abstr Pap Am Chem Soc 211, 121-ANYL
17. Odum JR, Hoffmann T, Bowman F, Collins D, Flagan RC, Seinfeld JH (1996) Gas/particle partitioning and secondary organic aerosol yields. Environ Sci Technol 30(8):2580–2585
18. Pankow JF (1994) An absorption-model of gas-particle partitioning of organic-compounds in the atmosphere. Atmos Environ 28(2):185–188

19. Liousse C, Penner JE, Chuang C, Walton JJ, Eddleman H, Cachier H (1996) A global three-dimensional model study of carbonaceous aerosols. J Geophys Res Atmos 101 (D14):19411–19432
20. Lurmann FW, Wexler AS, Pandis SN, Musarra S, Kumar N, Seinfeld JH (1997) Modelling urban and regional aerosols. 2. Application to California's south coast air basin. Atmos Environ 31:2695–2715
21. Griffin RJ, Cocker DR, Seinfeld JH, Dabdub D (1999) Estimate of global atmospheric organic aerosol from oxidation of biogenic hydrocarbons. Geophys Res Lett 26 (17):2721–2724
22. Pun BK, Griffin RJ, Seigneur C, Seinfeld JH (2002) Secondary organic aerosol - 2. Thermodynamic model for gas/particle partitioning of molecular constituents. J Geophys Res Atmos 107(D17):D4333. doi:10.1029/2001jd000542
23. Koo BY, Ansari AS, Pandis SN (2003) Integrated approaches to modeling the organic and inorganic atmospheric aerosol components. Atmos Environ 37:4757–4768
24. Spracklen DV, Carslaw KS, Kulmala M, Kerminen VM, Sihto SL, Riipinen I, Merikanto J, Mann GW, Chipperfield MP, Wiedensohler A, Birmili W, Lihavainen H (2008) Contribution of particle formation to global cloud condensation nuclei concentrations. Geophys Res Lett 35(6):L06808. doi:10.1029/2007gl033038
25. Heald CL, Ridley DA, Kreidenweis SM, Drury EE (2010) Satellite observations cap the atmospheric organic aerosol budget. Geophys Res Lett 37:L24808. doi:10.1029/2010gl045095
26. Novakov T, Penner JE (1993) Large contribution of organic aerosols to cloud-condensation-nuclei concentrations. Nature 365(6449):823–826
27. Cruz CN, Pandis SN (1997) A study of the ability of pure secondary organic aerosol to act as cloud condensation nuclei. Atmos Environ 31:2205–2214
28. Huff Hartz KE, Tischuk JE, Chan MN, Chan CK, Donahue NM, Pandis SN (2006) Cloud condensation nuclei activation of limited solubility organic aerosol. Atmos Environ 40:605–617
29. Huffman JA, Docherty KS, Aiken AC, Cubison MJ, Ulbrich IM, DeCarlo PF, Sueper D, Jayne JT, Worsnop DR, Zieann PJ, Jimenez JL (2009) Chemically-resolved aerosol volatility measurements from two megacity field studies. Atmos Chem Phys 9:7161–7182
30. Jimenez JL, Canagaratna MR, Donahue NM, Prevot ASH, Zhang Q, Kroll JH, DeCarlo PF, Allan JD, Coe H, Ng NL, Aiken AC, Docherty KS, Ulbrich IM, Grieshop AP, Robinson AL, Duplissy J, Smith JD, Wilson KR, Lanz VA, Hueglin C, Sun YL, Tian J, Laaksonen A, Raatikainen T, Rautiainen J, Vaattovaara P, Ehn M, Kulmala M, Tomlinson JM, Collins DR, Cubison MJ, Dunlea EJ, Huffman JA, Onasch TB, Alfarra MR, Williams PI, Bower K, Kondo Y, Schneider J, Drewnick F, Borrmann S, Weimer S, Demerjian K, Salcedo D, Cottrell L, Griffin R, Takami A, Miyoshi T, Hatakeyama S, Shimono A, Sun JY, Zhang YM, Dzepina K, Kimmel JR, Sueper D, Jayne JT, Herndon SC, Trimborn AM, Williams LR, Wood EC, Middlebrook AM, Kolb CE, Baltensperger U, Worsnop DR (2009) Evolution of organic aerosols in the atmosphere. Science 326(5959):1525–1529. doi:10.1126/science.1180353
31. Vaden TD, Imre D, Beranek J, Shrivastava M, Zelenyuk A (2011) Evaporation kinetics and phase of laboratory and ambient secondary organic aerosol. Proc Natl Acad Sci USA 108 (6):2190–2195
32. Zobrist B, Marcolli C, Pedernera DA, Koop T (2008) Do atmospheric aerosols form glasses? Atmos Chem Phys 8(17):5221–5244
33. Virtanen A, Joutsensaari J, Koop T, Kannosto J, Yli-Pirila P, Leskinen J, Makela JM, Holopainen JK, Poschl U, Kulmala M, Worsnop DR, Laaksonen A (2010) An amorphous solid state of biogenic secondary organic aerosol particles. Nature 467(7317):824–827
34. Koop T, Bookhold J, Shiraiwa M, Poschl U (2011) Glass transition and phase state of organic compounds: dependency on molecular properties and implications for secondary organic aerosols in the atmosphere. Phys Chem Chem Phys 13(43):19238–19255

35. Goldstein AH, Galbally IE (2007) Known and unexplored organic constituents in the Earth's atmosphere. Environ Sci Technol 41(5):1514–1521
36. Hallquist M, Wenger JC, Baltensperger U, Rudich Y, Simpson D, Claeys M, Dommen J, Donahue NM, George C, Goldstein AH, Hamilton JF, Herrmann H, Hoffmann T, Iinuma Y, Jang M, Jenkin ME, Jimenez JL, Kiendler-Scharr A, Maenhaut W, McFiggans G, Mentel TF, Monod A, Prevot ASH, Seinfeld JH, Surratt JD, Szmigielski R, Wildt J (2009) The formation, properties and impact of secondary organic aerosol: current and emerging issues. Atmos Chem Phys 9(14):5155–5236
37. Spracklen DV, Jimenez JL, Carslaw KS, Worsnop DR, Evans MJ, Mann GW, Zhang Q, Canagaratna MR, Allan J, Coe H, McFiggans G, Rap A, Forster P (2011) Aerosol mass spectrometer constraint on the global secondary organic aerosol budget. Atmos Chem Phys 11(23):12109–12136. doi:10.5194/acp-11-12109-2011
38. Donahue NM, Robinson AL, Pandis SN (2009) Atmospheric organic particulate matter: from smoke to secondary organic aerosol. Atmos Environ 43(1):94–106. doi:10.1016/j.atmosenv.2008.09.055
39. Marcolli C, Luo BP, Peter T, Wienhold FG (2004) Internal mixing of the organic aerosol by gas phase diffusion of semivolatile organic compounds. Atmos Chem Phys 4:2593–2599
40. Donahue NM, Robinson AL, Stanier CO, Pandis SN (2006) Coupled partitioning, dilution, and chemical aging of semivolatile organics. Environ Sci Technol 40:2635–2643
41. Aumont B, Szopa S, Madronich S (2005) Modelling the evolution of organic carbon during its gas-phase tropospheric oxidation: development of an explicit model based on a self generating approach. Atmos Chem Phys 5:2497–2517
42. Fredenslund A, Jones RL, Prausnitz JM (1975) Group-contribution estimation of activity-coefficients in nonideal liquid-mixtures. Aiche J 21(6):1086–1099
43. Clegg SL, Seinfeld JH, Brimblecombe P (2001) Thermodynamic modelling of aqueous aerosols containing electrolytes and dissolved organic compounds. J Aerosol Sci 32(6): 713–738
44. Nannoolal Y, Rarey J, Ramjugernath D (2008) Estimation of pure component properties - Part 3. Estimation of the vapor pressure of non-electrolyte organic compounds via group contributions and group interactions. Fluid Phase Equilib 269(1–2):117–133
45. Zuend A, Marcolli C, Booth AM, Lienhard DM, Soonsin V, Krieger UK, Topping DO, McFiggans G, Peter T, Seinfeld JH (2011) New and extended parameterization of the thermodynamic model AIOMFAC: calculation of activity coefficients for organic–inorganic mixtures containing carboxyl, hydroxyl, carbonyl, ether, ester, alkenyl, alkyl, and aromatic functional groups. Atmos Chem Phys 11(17):9155–9206
46. Chen Q, Liu YJ, Donahue NM, Shilling JE, Martin ST (2011) Particle-phase chemistry of secondary organic material: modeled compared to measured O:C and H:C elemental ratios provide constraints. Environ Sci Technol 45(11):4763–4770
47. Xia AG, Michelangeli DV, Makar PA (2008) Box model studies of the secondary organic aerosol formation under different HC/NO(x) conditions using the subset of the Master Chemical Mechanism for alpha-pinene oxidation. J Geophys Res Atmos 113:D10
48. Capouet M, Mueller JF, Ceulemans K, Compernolle S, Vereecken L, Peeters J (2008) Modeling aerosol formation in alpha-pinene photo-oxidation experiments. J Geophys Res Atmos 113(D2):D02308
49. Valorso R, Aumont B, Camredon M, Raventos-Duran T, Mouchel-Vallon C, Ng NL, Seinfeld JH, Lee-Taylor J, Madronich S (2011) Explicit modelling of SOA formation from alpha-pinene photooxidation: sensitivity to vapour pressure estimation. Atmos Chem Phys 11(14):6895–6910
50. Pun BK, Wu SY, Seigneur C, Seinfeld JH, Griffin RJ, Pandis SN (2003) Uncertainties in modeling secondary organic aerosols: three-dimensional modeling studies in Nashville/Western Tennessee. Environ Sci Technol 37:3647–3661
51. Kroll JH, Seinfeld JH (2008) Chemistry of secondary organic aerosol: formation and evolution of low-volatility organics in the atmosphere. Atmos Environ 42(16):3593–3624

52. Kroll JH, Ng NL, Murphy SM, Flagan RC, Seinfeld JH (2006) Secondary organic aerosol formation from isoprene photooxidation. Environ Sci Technol 40(6):1869–1877. doi:Doi 10.1021/Es0524301
53. Griffin RJ, Cocker DR, Flagan RC, Seinfeld JH (1999) Organic aerosol formation from the oxidation of biogenic hydrocarbons. J Geophys Res Atmos 104(D3):3555–3567
54. Presto AA, Huff Hartz KE, Donahue NM (2005) Secondary organic aerosol production from terpene ozonolysis. 2. Effect of NOx concentration. Environ Sci Technol 39:7046–7054
55. Barsanti KC, Smith JN, Pankow JF (2011) Application of the np plus mP modeling approach for simulating secondary organic particulate matter formation from alpha-pinene oxidation. Atmos Environ 45(37):6812–6819
56. Grieshop AP, Miracolo MA, Donahue NM, Robinson AL (2009) Constraining the volatility distribution and gas-particle partitioning of combustion aerosols using isothermal dilution and thermodenuder measurements. Environ Sci Technol 43(13):4750–4756. doi:10.1021/es8032378
57. Dommen J, Hellen H, Saurer M, Jaeggi M, Siegwolf R, Metzger A, Duplissy J, Fierz M, Baltensperger U (2009) Determination of the aerosol yield of isoprene in the presence of an organic seed with carbon isotope analysis. Environ Sci Technol 43(17):6697–6702
58. Hildebrandt L, Henry KM, Kroll JH, Worsnop DR, Pandis SN, Donahue NM (2011) Evaluating the mixing of organic aerosol components using high-resolution aerosol mass spectrometry. Environ Sci Technol 45(15):6329–6335
59. Song C, Zaveri RA, Alexander ML, Thornton JA, Madronich S, Ortega JV, Zelenyuk A, Yu X-Y, Laskin A, Maughan DA (2007) Effect of hydrophobic primary organic aerosols on secondary organic aerosol formation from ozonolysis of alpha-pinene. Geophys Res Lett 34 (20):L20803
60. Asa-Awuku A, Miracolo MA, Kroll JH, Robinson AL, Donahue NM (2009) Mixing and phase partitioning of primary and secondary organic aerosols. Geophys Res Lett 36:L15827. doi:10.1029/2009gl039301
61. Pankow JF, Barsanti KC (2009) The carbon number-polarity grid: a means to manage the complexity of the mix of organic compounds when modeling atmospheric organic particulate matter. Atmos Environ 43(17):2829–2835
62. Simoneit BRT, Schauer JJ, Nolte CG, Oros DR, Elias VO, Fraser MP, Rogge WF, Cass GR (1999) Levoglucosan, a tracer for cellulose in biomass burning and atmospheric particles. Atmos Environ 33(2):173–182
63. Donahue NM, Epstein SA, Pandis SN, Robinson AL (2011) A two-dimensional volatility basis set: 1. organic-aerosol mixing thermodynamics. Atmos Chem Phys 11(7):3303–3318
64. Donahue NM, Kroll JH, Pandis SN, Robinson AL (2012) A two-dimensional volatility basis set – part 2: diagnostics of organic-aerosol evolution. Atmos Chem Phys 12:615–634. doi:10.5194/acp-12-615-2012
65. Kroll JH, Donahue NM, Jimenez JL, Kessler SH, Canagaratna MR, Wilson KR, Altieri KE, Mazzoleni LR, Wozniak AS, Bluhm H, Mysak ER, Smith JD, Kolb CE, Worsnop DR (2011) Carbon oxidation state as a metric for describing the chemistry of atmospheric organic aerosol. Nat Chem 3(2):133–139. doi:10.1038/nchem.948
66. Heald CL, Kroll JH, Jimenez JL, Docherty KS, DeCarlo PF, Aiken AC, Chen Q, Martin ST, Farmer DK, Artaxo P (2010) A simplified description of the evolution of organic aerosol composition in the atmosphere. Geophys Res Lett 37:L08803. doi:10.1029/2010gl042737
67. Aiken AC, Decarlo PF, Kroll JH, Worsnop DR, Huffman JA, Docherty KS, Ulbrich IM, Mohr C, Kimmel JR, Sueper D, Sun Y, Zhang Q, Trimborn A, Northway M, Ziemann PJ, Canagaratna MR, Onasch TB, Alfarra MR, Prevot ASH, Dommen J, Duplissy J, Metzger A, Baltensperger U, Jimenez JL (2008) O/C and OM/OC ratios of primary, secondary, and ambient organic aerosols with high-resolution time-of-flight aerosol mass spectrometry. Environ Sci Technol 42(12):4478–4485

68. Epstein SA, Riipinen I, Donahue NM (2010) A semiempirical correlation between enthalpy of vaporization and saturation concentration for organic aerosol. Environ Sci Technol 44 (2):743–748. doi:10.1021/es902497z
69. Cappa CD, Jimenez JL (2010) Quantitative estimates of the volatility of ambient organic aerosol. Atmos Chem Phys 10(12):5409–5424
70. Kulmala M, Toivonen A, Makela JM, Laaksonen A (1998) Analysis of the growth of nucleation mode particles observed in boreal forest. Tellus B Chem Phys Meteorol 50 (5):449–462
71. Anttila T, Kerminen VM, Kulmala M, Laaksonen A, O'Dowd CD (2004) Modelling the formation of organic particles in the atmosphere. Atmos Chem Phys 4:1071–1083
72. Riipinen I, Manninen HE, Yli-Juuti T, Boy M, Sipila M, Ehn M, Junninen H, Petaja T, Kulmala M (2009) Applying the condensation particle counter battery (CPCB) to study the water-affinity of freshly-formed 2–9 nm particles in boreal forest. Atmos Chem Phys 9 (10):3317–3330
73. Riipinen I, Pierce JR, Yli-Juuti T, Nieminen T, Hakkinen S, Ehn M, Junninen H, Lehtipalo K, Petaja T, Slowik J, Chang R, Shantz NC, Abbatt J, Leaitch WR, Kerminen VM, Worsnop DR, Pandis SN, Donahue NM, Kulmala M (2011) Organic condensation: a vital link connecting aerosol formation to cloud condensation nuclei (CCN) concentrations. Atmos Chem Phys 11 (8):3865–3878. doi:10.5194/acp-11-3865-2011
74. Pierce JR, Riipinen I, Kulmala M, Ehn M, Petaja T, Junninen H, Worsnop DR, Donahue NM (2011) Quantification of the volatility of secondary organic compounds in ultrafine particles during nucleation events. Atmos Chem Phys 11(17):9019–9036
75. Donahue NM, Trump ER, Pierce JR, Riipinen I (2011) Theoretical constraints on pure vapor-pressure driven condensation of organics to ultrafine particles. Geophys Res Lett 38:L16801
76. Wexler AS, Lurmann FW, Seinfeld JH (1994) Modeling urban and regional aerosols. 1. Model development. Atmos Environ 28(3):531–546
77. Riipinen I, Pierce JR, Donahue NM, Pandis SN (2010) Equilibration time scales of organic aerosol inside thermodenuders: evaporation kinetics versus thermodynamics. Atmos Environ 44(5):597–607. doi:10.1016/j.atmosenv.2009.11.022
78. Worsnop DR, Zahniser MS, Kolb CE, Gardner JA, Watson LR, Vandoren JM, Jayne JT, Davidovits P (1989) Temperature-dependence of mass accommodation of So2 and H2o2 on aqueous surfaces. J Phys Chem 93(3):1159–1172
79. Ammann M, Pöschl U, Rudich Y (2003) Effects of reversible adsorption and Langmuir-Hinshelwood surface reactions on gas uptake by atmospheric particles. Phys Chem Chem Phys 5(2):351–356
80. Davidovits P, Worsnop DR, Jayne JT, Kolb CE, Winkler P, Vrtala A, Wagner PE, Kulmala M, Lehtinen KEJ, Vesala T, Mozurkewich M (2004) Mass accommodation coefficient of water vapor on liquid water. Geophys Res Lett 31(22):L22111. doi:10.1029/2004gl020835
81. Smith JD, Cappa CD, Drisdell WS, Cohen RC, Saykally RJ (2006) Raman thermometry measurements of free evaporation from liquid water droplets. J Am Chem Soc 128 (39):12892–12898
82. Laaksonen A, Vesala T, Kulmala M, Winkler PM, Wagner PE (2005) Commentary on cloud modelling and the mass accommodation coefficient of water. Atmos Chem Phys 5:461–464
83. Winkler PM, Vrtala A, Wagner PE, Kulmala M, Lehtinen KEJ, Vesala T (2004) Mass and thermal accommodation during gas–liquid condensation of water. Phys Rev Lett 93(7): 075701
84. Kolb CE, Cox RA, Abbatt JPD, Ammann M, Davis EJ, Donaldson DJ, Garrett BC, George C, Griffiths PT, Hanson DR, Kulmala M, McFiggans G, Poschl U, Riipinen I, Rossi MJ, Rudich Y, Wagner PE, Winkler PM, Worsnop DR, O' Dowd CD (2010) An overview of current issues in the uptake of atmospheric trace gases by aerosols and clouds. Atmos Chem Phys 10(21):10561–10605

85. Nogueira JJ, Vazquez SA, Mazyar OA, Hase WL, Perkins BG, Nesbitt DJ, Martinez-Nunez E (2009) Dynamics of CO(2) scattering off a perfluorinated self-assembled monolayer. Influence of the incident collision energy, mass effects, and use of different surface models. J Phys Chem A 113(16):3850–3865
86. Saleh R, Khlystov A, Shihadeh A (2012) Determination of evaporation coefficients of ambient and laboratory-generated semivolatile organic aerosols from phase equilibration kinetics in a thermodenuder. Aerosol Sci Technol 46(1):22–30
87. Shiraiwa M, Ammann M, Koop T, Poschl U (2011) Gas uptake and chemical aging of semisolid organic aerosol particles. Proc Natl Acad Sci USA 108(27):11003–11008
88. Lanz VA, Alfarra MR, Baltensperger U, Buchmann B, Hueglin C, Szidat S, Wehrli MN, Wacker L, Weimer S, Caseiro A, Puxbaum H, Prevot ASH (2008) Source attribution of submicron organic aerosols during wintertime inversions by advanced factor analysis of aerosol mass spectra. Environ Sci Technol 42(1):214–220
89. Fraser MP, Cass GR, Simoneit BRT, Rasmussen RA (1997) Air quality model evaluation data for organics .4. C-2-C-36 non-aromatic hydrocarbons. Environ Sci Technol 31(8): 2356–2367
90. Robinson AL, Grieshop AP, Donahue NM, Hunt SW (2010) Updating the conceptual model for fine particle mass emissions from combustion systems. J Air Waste Manag Assoc 60 (10):1204–1222. doi:10.3155/1047-3289.60.10.1204
91. Williams BJ, Goldstein AH, Kreisberg NM, Hering SV (2006) An in-situ instrument for speciated organic composition of atmospheric aerosols: thermal desorption aerosol GC/MS-FID (TAG). Aerosol Sci Technol 40(8):627–638. doi:Doi 10.1080/02786820600754631
92. Lambe AT, Miracolo MA, Hennigan CJ, Robinson AL, Donahue NM (2009) Effective rate constants and uptake coefficients for the reactions of organic molecular markers (n-alkanes, hopanes, and steranes) in motor oil and diesel primary organic aerosols with hydroxyl radicals. Environ Sci Technol 43(23):8794–8800. doi:10.1021/es901745h
93. Miracolo MA, Presto AA, Lambe AT, Hennigan CJ, Donahue NM, Kroll JH, Worsnop DR, Robinson AL (2010) Photo-oxidation of low-volatility organics found in motor vehicle emissions: production and chemical evolution of organic aerosol mass. Environ Sci Technol 44(5):1638–1643. doi:10.1021/es902635c
94. Shrivastava MK, Lipsky EM, Stanier CO, Robinson AL (2006) Modeling semivolatile organic aerosol mass emissions from combustion systems. Environ Sci Technol 40:2671–2677
95. Fraser MP, Cass GR, Simoneit BRT (1998) Gas-phase and particle-phase organic compounds emitted from motor vehicle traffic in a Los Angeles roadway tunnel. Environ Sci Technol 32 (14):2051–2060
96. Yokelson RJ, Crounse JD, DeCarlo PF, Karl T, Urbanski S, Atlas E, Campos T, Shinozuka Y, Kapustin V, Clarke AD, Weinheimer A, Knapp DJ, Montzka DD, Holloway J, Weibring P, Flocke F, Zheng W, Toohey D, Wennberg PO, Wiedinmyer C, Mauldin L, Fried A, Richter D, Walega J, Jimenez JL, Adachi K, Buseck PR, Hall SR, Shetter R (2009) Emissions from biomass burning in the Yucatan. Atmos Chem Phys 9(15):5785–5812
97. Zhang KM, Wexler AS (2004) Evolution of particle number distribution near roadways - part I: analysis of aerosol dynamics and its implications for engine emission measurement. Atmos Environ 38(38):6643–6653
98. Zhang Y, Liu P, Liu XH, Jacobson MZ, McMurry PH, Yu FQ, Yu SC, Schere KL (2010) A comparative study of nucleation parameterizations: 2. Three-dimensional model application and evaluation. J Geophys Res Atmos 115:D20213
99. Guenther A, Hewitt CN, Erickson D, Fall R, Geron C, Graedel T, Harley P, Klinger L, Lerdau M, McKay WA, Pierce T, Scholes B, Steinbrecher R, Tallamraju R, Taylor J, Zimmerman P (1995) A global-model of natural volatile organic-compound emissions. J Geophys Res Atmos 100(D5):8873–8892. doi:10.1029/94jd02950
100. Jaoui M, Kamens RM (2001) Mass balance of gaseous and particulate products analysis from alpha-pinene/NOx/air in the presence of natural sunlight. J Geophys Res Atmos 106 (D12):12541–12558

101. Presto AA, Huff Hartz KE, Donahue NM (2005) Secondary organic aerosol production from terpene ozonolysis. 1. Effect of UV radiation. Environ Sci Technol 39:7036–7045
102. Isaacman G, Worton DR, Kreisberg NM, Hennigan CJ, Teng AP, Hering SV, Robinson AL, Donahue NM, Goldstein AH (2011) Understanding evolution of product composition and volatility distribution through in-situ GC x GC analysis: a case study of longifolene ozonolysis. Atmos Chem Phys 11(11):5335–5346
103. Tolocka MP, Jang M, Ginter JM, Cox FJ, Kamens RM, Johnston MV (2004) Formation of oligomers in secondary organic aerosol. Environ Sci Technol 38(5):1428–1434. doi:Doi 10.1021/Es035030r
104. Baltensperger U, Kalberer M, Dommen J, Paulsen D, Alfarra MR, Coe H, Fisseha R, Gascho A, Gysel M, Nyeki S, Sax M, Steinbacher M, Prevot ASH, Sjogren S, Weingartner E, Zenobi R (2005) Secondary organic aerosols from anthropogenic and biogenic precursors. Faraday Discuss 130:265–278. doi:Doi 10.1039/B417367h
105. Hall WA, Johnston MV (2011) Oligomer content of alpha-pinene secondary organic aerosol. Aerosol Sci Technol 45(1):37–45
106. Surratt JD, Kroll JH, Kleindienst TE, Edney EO, Claeys M, Sorooshian A, Ng NL, Offenberg JH, Lewandowski M, Jaoui M, Flagan RC, Seinfeld JH (2007) Evidence for organosulfates in secondary organic aerosol. Environ Sci Technol 41(2):517–527
107. Kroll JH, Seinfeld JH (2005) Representation of secondary organic aerosol laboratory chamber data for the interpretation of mechanisms of particle growth. Environ Sci Technol 39(11):4159–4165. doi:Doi 10.1021/Es048292h
108. Grieshop AP, Donahue NM, Robinson AL (2007) Is the gas-particle partitioning in alpha-pinene secondary organic aerosol reversible? Geophys Res Lett 34(14):L14810. doi:10.1029/2007gl029987
109. An WJ, Pathak RK, Lee BH, Pandis SN (2007) Aerosol volatility measurement using an improved thermodenuder: application to secondary organic aerosol. J Aerosol Sci 38(3):305–314. doi:10.1016/j.jaerosci.2006.12.002
110. Huffman JA, Ziemann PJ, Jayne JT, Worsnop DR, Jimenez JL (2008) Development and characterization of a fast-stepping/scanning thermodenuder for chemically-resolved aerosol volatility measurements. Aerosol Sci Technol 42(5):395–407
111. Lee BH, Pierce JR, Engelhart GJ, Pandis SN (2011) Volatility of secondary organic aerosol from the ozonolysis of monoterpenes. Atmos Environ 45(14):2443–2452. doi:10.1016/j.atmosenv.2011.02.004
112. Tritscher T, Dommen J, DeCarlo PF, Gysel M, Barmet PB, Praplan AP, Weingartner E, Prévôt ASH, Riipinen I, Donahue NM, Baltensperger U (2011) Volatility and hygroscopicity of aging secondary organic aerosol in a smog chamber. Atmos Chem Phys 11(22):11477–11496. doi:10.5194/acp-11-11477-2011
113. Salo K, Hallquist M, Jonsson AM, Saathoff H, Naumann KH, Spindler C, Tillmann R, Fuchs H, Bohn B, Rubach F, Mentel TF, Muller L, Reinnig M, Hoffmann T, Donahue NM (2011) Volatility of secondary organic aerosol during OH radical induced ageing. Atmos Chem Phys 11(21):11055–11067
114. Kostenidou E, Lee BH, Engelhart GJ, Pierce JR, Pandis SN (2009) Mass spectra deconvolution of low, medium, and high volatility biogenic secondary organic aerosol. Environ Sci Technol 43(13):4884–4889. doi:10.1021/es803676g
115. Lee BH, Kostenidou E, Hildebrandt L, Riipinen I, Engelhart GJ, Mohr C, DeCarlo PF, Mihalopoulos N, Prevot ASH, Baltensperger U, Pandis SN (2010) Measurement of the ambient organic aerosol volatility distribution: application during the Finokalia Aerosol Measurement Experiment (FAME-2008). Atmos Chem Phys 10(24):12149–12160. doi:10.5194/acp-10-12149-2010
116. Simoneit BRT (2002) Biomass burning - a review of organic tracers for smoke from incomplete combustion. Appl Geochem 17(3):129–162
117. Chan MN, Surratt JD, Claeys M, Edgerton ES, Tanner RL, Shaw SL, Zheng M, Knipping EM, Eddingsaas NC, Wennberg PO, Seinfeld JH (2010) Characterization and quantification of isoprene-derived epoxydiols in ambient aerosol in the southeastern United States. Environ Sci Technol 44(12):4590–4596

118. Ervens B, Turpin BJ, Weber RJ (2011) Secondary organic aerosol formation in cloud droplets and aqueous particles (aqSOA): a review of laboratory, field and model studies. Atmos Chem Phys 11(21):11069–11102
119. Maria SF, Russell LM, Gilles MK, Myneni SCB (2004) Organic aerosol growth mechanisms and their climate-forcing implications. Science 306(5703):1921–1924
120. Seinfeld JH, Pandis SN (2006) Atmospheric chemistry and physics, 2nd edn. Wiley, Hoboken
121. Kroll JH, Chan AWH, Ng NL, Flagan RC, Seinfeld JH (2007) Reactions of semivolatile organics and their effects on secondary organic aerosol formation. Environ Sci Technol 41 (10):3545–3550
122. Pathak R, Donahue NM, Pandis SN (2008) Ozonolysis of beta-pinene: temperature dependence of secondary organic aerosol mass fraction. Environ Sci Technol 42(14):5081–5086. doi:10.1021/es070721z
123. Hildebrandt L, Donahue NM, Pandis SN (2009) High formation of secondary organic aerosol from the photo-oxidation of toluene. Atmos Chem Phys 9(9):2973–2986
124. Prisle NL, Engelhart GJ, Bilde M, Donahue NM (2010) Humidity influence on gas-particle phase partitioning of alpha-pinene + O(3) secondary organic aerosol. Geophys Res Lett 37:5. doi:10.1029/2009gl041402
125. Bertram AK, Martin ST, Hanna SJ, Smith ML, Bodsworth A, Chen Q, Kuwata M, Liu A, You Y, Zorn SR (2011) Predicting the relative humidities of liquid-liquid phase separation, efflorescence, and deliquescence of mixed particles of ammonium sulfate, organic material, and water using the organic-to-sulfate mass ratio of the particle and the oxygen-to-carbon elemental ratio of the organic component. Atmos Chem Phys 11(21):10995–11006
126. Zuend A, Marcolli C, Peter T, Seinfeld JH (2010) Computation of liquid-liquid equilibria and phase stabilities: implications for RH-dependent gas/particle partitioning of organic–inorganic aerosols. Atmos Chem Phys 10(16):7795–7820
127. Robinson AL, Donahue NM, Shrivastava MK, Weitkamp EA, Sage AM, Grieshop AP, Lane TE, Pierce JR, Pandis SN (2007) Rethinking organic aerosols: semivolatile emissions and photochemical aging. Science 315(5816):1259–1262
128. Weitkamp EA, Sage AM, Pierce JR, Donahue NM, Robinson AL (2007) Organic aerosol formation from photochemical oxidation of diesel exhaust in a smog chamber. Environ Sci Technol 41(20):6969–6975
129. Sage AM, Weitkamp EA, Robinson AL, Donahue NM (2008) Evolving mass spectra of the oxidized component of organic aerosol: results from aerosol mass spectrometer analyses of aged diesel emissions. Atmos Chem Phys 8(5):1139–1152
130. Zhang Q, Alfarra MR, Worsnop DR, Allan JD, Coe H, Canagaratna MR, Jimenez JL (2005) Deconvolution and quantification of hydrocarbon-like and oxygenated organic aerosols based on aerosol mass spectrometry. Environ Sci Technol 39(13):4938–4952
131. Shilling JE, Chen Q, King SM, Rosenoern T, Kroll JH, Worsnop DR, DeCarlo PF, Aiken AC, Sueper D, Jimenez JL, Martin ST (2009) Loading-dependent elemental composition of alpha-pinene SOA particles. Atmos Chem Phys 9(3):771–782
132. Lim YB, Ziemann PJ (2005) Products and mechanism of secondary organic aerosol formation from reactions of n-alkanes with OH radicals in the presence of NOx. Environ Sci Technol 39(23):9229–9236
133. Presto AA, Miracolo MA, Donahue NM, Robinson AL (2010) Secondary organic aerosol formation from high-NO(x) photo-oxidation of low volatility precursors: n-alkanes. Environ Sci Technol 44(6):2029–2034. doi:10.1021/es903712r
134. Lim YB, Ziemann PJ (2009) Effects of molecular structure on aerosol yields from OH radical-initiated reactions of linear, branched, and cyclic alkanes in the presence of NOx. Environ Sci Technol 43(7):2328–2334
135. Pitts JN, Vancauwenberghe KA, Grosjean D, Schmid JP, Fitz DR, Belser WL, Knudson GB, Hynds PM (1978) Atmospheric reactions of polycyclic aromatic-hydrocarbons - facile formation of mutagenic nitro-derivatives. Science 202(4367):515–519

136. Kamens RM, Fulcher JN, Zhishi G (1986) Effects of temperature on wood soot pah decay in atmospheres with sunlight and low Nox. Atmos Environ 20(8):1579–1587
137. Pankow JF, Isabelle LM, Buchholz DA, Luo WT, Reeves BD (1994) Gas-particle partitioning of polycyclic aromatic-hydrocarbons and alkanes to environmental tobacco-smoke. Environ Sci Technol 28(2):363
138. Pankow JF (1987) Review and comparative-analysis of the theories on partitioning between the gas and aerosol particulate phases in the atmosphere. Atmos Environ 21(11): 2275–2283
139. Pankow JF (1991) Common gamma-intercept and single compound regressions of gas particle partitioning data vs 1/T. Atmos Environ Part A General Topics 25(10):2229–2239
140. Pankow JF (1994) An absorption-model of the gas aerosol partitioning involved in the formation of secondary organic aerosol. Atmos Environ 28(2):189–193
141. Chan AWH, Kautzman KE, Chhabra PS, Surratt JD, Chan MN, Crounse JD, Kurten A, Wennberg PO, Flagan RC, Seinfeld JH (2009) Secondary organic aerosol formation from photooxidation of naphthalene and alkylnaphthalenes: implications for oxidation of intermediate volatility organic compounds (IVOCs). Atmos Chem Phys 9(9):3049–3060
142. Rogge WF, Hildemann LM, Mazurek MA, Cass GR, Simoneit BRT (1996) Mathematical modeling of atmospheric fine particle-associated primary organic compound concentrations. J Geophys Res Atmos 101(D14):19379–19394
143. Weitkamp EA, Lambe AT, Donahue NM, Robinson AL (2008) Laboratory measurements of the heterogeneous oxidation of condensed-phase organic molecular makers for motor vehicle exhaust. Environ Sci Technol 42(21):7950–7956. doi:10.1021/es800745x
144. Chirico R, DeCarlo PF, Heringa MF, Tritscher T, Richter R, Prevot ASH, Dommen J, Weingartner E, Wehrle G, Gysel M, Laborde M, Baltensperger U (2010) Impact of aftertreatment devices on primary emissions and secondary organic aerosol formation potential from in-use diesel vehicles: results from smog chamber experiments. Atmos Chem Phys 10(23):11545–11563
145. Grieshop AP, Donahue NM, Robinson AL (2009) Laboratory investigation of photochemical oxidation of organic aerosol from wood fires 2: analysis of aerosol mass spectrometer data. Atmos Chem Phys 9(6):2227–2240
146. Heringa MF, DeCarlo PF, Chirico R, Tritscher T, Dommen J, Weingartner E, Richter R, Wehrle G, Prevot ASH, Baltensperger U (2011) Investigations of primary and secondary particulate matter of different wood combustion appliances with a high-resolution time-of-flight aerosol mass spectrometer. Atmos Chem Phys 11(12):5945–5957
147. Miracolo MA, Hennigan CJ, Ranjan M, Nguyen NT, Gordon TD, Lipsky EM, Presto AA, Donahue NM, Robinson AL (2011) Secondary aerosol formation from photochemical aging of aircraft exhaust in a smog chamber. Atmos Chem Phys 11(9):4135–4147
148. Hennigan CJ, Sullivan AP, Collett JL, Robinson AL (2010) Levoglucosan stability in biomass burning particles exposed to hydroxyl radicals. Geophys Res Lett 37:L09806. doi:10.1029/2010gl043088
149. Ng NL, Kroll JH, Keywood MD, Bahreini R, Varutbangkul V, Flagan RC, Seinfeld JH, Lee A, Goldstein AH (2006) Contribution of first- versus second-generation products to secondary organic aerosols formed in the oxidation of biogenic hydrocarbons. Environ Sci Technol 40(7):2283–2297
150. Zhang JY, Hartz KEH, Pandis SN, Donahue NM (2006) Secondary organic aerosol formation from limonene ozonolysis: homogeneous and heterogeneous influences as a function of NOx. J Phys Chem A 110(38):11053–11063
151. Leungsakul S, Jaoui M, Kamens RM (2005) Kinetic mechanism for predicting secondary organic aerosol formation from the reaction of d-limonene with ozone. Environ Sci Technol 39(24):9583–9594
152. Donahue NM, Tischuk JE, Marquis BJ, Huff Hartz KE (2007) Secondary organic aerosol from limona ketone: insights into terpene ozonolysis via synthesis of key intermediates. Phys Chem Chem Phys 9(23):2991–2998

153. Maksymiuk CS, Gayahtri C, Gil RR, Donahue NM (2009) Secondary organic aerosol formation from multiphase oxidation of limonene by ozone: mechanistic constraints via two-dimensional heteronuclear NMR spectroscopy. Phys Chem Chem Phys 11(36): 7810–7818. doi:10.1039/b820005j
154. Claeys M, Szmigielski R, Kourtchev I, Van der Veken P, Vermeylen R, Maenhaut W, Jaoui M, Kleindienst TE, Lewandowski M, Offenberg JH, Edney EO (2007) Hydroxydicarboxylic acids: markers for secondary organic aerosol from the photooxidation of alpha-pinene. Environ Sci Technol 41(5):1628–1634
155. Mueller L, Reinnig MC, Naumann KH, Saathoff H, Mentel TF, Donahue NM, Hoffmann T (2012) Formation of 3-methyl-1,2,3-butanetricarboxylic acid via gas phase oxidation of pinonic acid - a mass spectrometric study of SOA aging. Atmos Chem Phys 12:1483–1496. doi:10.5194/acp-12-1483-2012
156. Chhabra PS, Ng NL, Canagaratna MR, Corrigan AL, Russell LM, Worsnop DR, Flagan RC, Seinfeld JH (2011) Elemental composition and oxidation of chamber organic aerosol. Atmos Chem Phys 11(17):8827–8845
157. Ng NL, Canagaratna MR, Zhang Q, Jimenez JL, Tian J, Ulbrich IM, Kroll JH, Docherty KS, Chhabra PS, Bahreini R, Murphy SM, Seinfeld JH, Hildebrandt L, Donahue NM, DeCarlo PF, Lanz VA, Prevot ASH, Dinar E, Rudich Y, Worsnop DR (2010) Organic aerosol components observed in northern hemispheric datasets from aerosol mass spectrometry. Atmos Chem Phys 10(10):4625–4641. doi:10.5194/acp-10-4625-2010
158. Donahue NM, Henry KM, Mentel TF, Scharr AK, Spindler C, Bohn B, Brauers T, Dorn HP, Fuchs H, Tillmann R, Wahner A, Saathoff H, Naumann KH, Möhler O, Leisner T, Müller L, Reinnig M-C, Hoffmann T, Salow K, Hallquist M, Frosch M, Bilde M, Tritscher T, Barmet P, Praplan AP, DeCarlo PF, Dommen J, Prévôt ASH, Baltensperger U (2012) Aging of biogenic secondary organic aerosol via gas-phase OH radical reactions. Proc Natl Acad Sci 109(34): 13503–13508. doi:10.1073/pnas.1115186109
159. Frosch M, Bilde M, DeCarlo PF, Juranyi Z, Tritscher T, Dommen J, Donahue NM, Gysel M, Weingartner E, Baltensperger U (2011) Relating cloud condensation nuclei activity and oxidation level of alpha-pinene secondary organic aerosols. J Geophys Res Atmos 116: D22212
160. Barmet P, Dommen J, DeCarlo PF, Tritscher T, Praplan AP, Platt SM, Prévôt ASH, Donahue NM, Baltensperger U (2012) OH clock determination by proton transfer reaction mass spectrometry at an environmental chamber. Atmos Meas Tech 5:7471–7498. doi:10.5194/amt-5-647-2012
161. Rudich Y, Donahue NM, Mentel TF (2007) Aging of organic aerosol: bridging the gap between laboratory and field studies. Annu Rev Phys Chem 58:321–352
162. Massoli P, Lambe AT, Ahern AT, Williams LR, Ehn M, Mikkila J, Canagaratna MR, Brune WH, Onasch TB, Jayne JT, Petaja T, Kulmala M, Laaksonen A, Kolb CE, Davidovits P, Worsnop DR (2011) Relationship between aerosol oxidation level and hygroscopic properties of laboratory generated secondary organic aerosol (SOA) particles (vol 37, L24801, 2010). Geophys Res Lett 38:L03805. doi:10.1029/2011gl046687
163. Hearn JD, Lovett AJ, Smith GD (2005) Ozonolysis of oleic acid particles: evidence for a surface reaction and secondary reactions involving Criegee intermediates. Phys Chem Chem Phys 7(3):501–511
164. Sage AM, Weitkamp EA, Robinson AL, Donahue NM (2009) Reactivity of oleic acid in organic particles: changes in oxidant uptake and reaction stoichiometry with particle oxidation. Phys Chem Chem Phys 11(36):7951–7962. doi:10.1039/b904285g
165. Donahue NM, Robinson AL, Hartz KEH, Sage AM, Weitkamp EA (2005) Competitive oxidation in atmospheric aerosols: the case for relative kinetics. Geophys Res Lett 32:L16805
166. Huff Hartz KE, Weitkamp EA, Sage AM, Donahue NM, Robinson AL (2007) Laboratory measurements of the oxidation kinetics of organic aerosol mixtures using a relative rate constants approach. J Geophys Res Atmos 112:D04204

167. Wagstrom KM, Pandis SN (2009) Determination of the age distribution of primary and secondary aerosol species using a chemical transport model. J Geophys Res Atmos 114: D14303. doi:10.1029/2009jd011784
168. Worsnop DR, Morris JW, Shi Q, Davidovits P, Kolb CE (2002) A chemical kinetic model for reactive transformations of aerosol particles. Geophys Res Lett 29(20):1996
169. Smith JD, Kroll JH, Cappa CD, Che DL, Liu CL, Ahmed M, Leone SR, Worsnop DR, Wilson KR (2009) The heterogeneous reaction of hydroxyl radicals with sub-micron squalane particles: a model system for understanding the oxidative aging of ambient aerosols. Atmos Chem Phys 9(9):3209–3222
170. Lim HJ, Carlton AG, Turpin BJ (2005) Isoprene forms secondary organic aerosol through cloud processing: model simulations. Environ Sci Technol 39(12):4441–4446
171. Lim YB, Tan Y, Perri MJ, Seitzinger SP, Turpin BJ (2010) Aqueous chemistry and its role in secondary organic aerosol (SOA) formation. Atmos Chem Phys 10(21):10521–10539
172. Ervens B, Volkamer R (2010) Glyoxal processing by aerosol multiphase chemistry: towards a kinetic modeling framework of secondary organic aerosol formation in aqueous particles. Atmos Chem Phys 10(17):8219–8244
173. Herrmann H, Hoffmann D, Schaefer T, Brauer P, Tilgner A (2010) Tropospheric aqueous-phase free-radical chemistry: radical sources, spectra. Reaction kinetics and prediction tools. Chemphyschem 11(18):3796–3822
174. Sander R (1999) Compilation of Henry's law constants for inorganic and organic species of potential importance in environmental chemistry. http://www.rolf-sander.net/henry/henry.pdf
175. Griffin RJ, Nguyen K, Dabdub D, Seinfeld JH (2003) A coupled hydrophobic-hydrophilic model for predicting secondary organic aerosol formation. J Atmos Chem 44(2):171–190
176. Volkamer R, Ziemann PJ, Molina MJ (2009) Secondary organic aerosol formation from acetylene (C(2)H(2)): seed effect on SOA yields due to organic photochemistry in the aerosol aqueous phase. Atmos Chem Phys 9(6):1907–1928
177. Galloway MM, Huisman AJ, Yee LD, Chan AWH, Loza CL, Seinfeld JH, Keutsch FN (2011) Yields of oxidized volatile organic compounds during the OH radical initiated oxidation of isoprene, methyl vinyl ketone, and methacrolein under high-NO(x) conditions. Atmos Chem Phys 11(21):10779–10790
178. DeCarlo PF, Dunlea EJ, Kimmel JR, Aiken AC, Sueper D, Crounse J, Wennberg PO, Emmons L, Shinozuka Y, Clarke A, Zhou J, Tomlinson J, Collins DR, Knapp D, Weinheimer AJ, Montzka DD, Campos T, Jimenez JL (2008) Fast airborne aerosol size and chemistry measurements above Mexico City and central Mexico during the MILAGRO campaign. Atmos Chem Phys 8(14):4027–4048
179. Hildebrandt L, Kostenidou E, Mihalopoulos N, Worsnop DR, Donahue NM, Pandis SN (2010) Formation of highly oxygenated organic aerosol in the atmosphere: insights from the Finokalia aerosol measurement experiments. Geophys Res Lett 37:L23801. doi:10.1029/2010gl045193